CZECH TECHNICAL UNIVERSITY IN PRAGUE

FACULTY OF BIOMEDICAL ENGINEERING

Department of Biomedical Technology

Design and development of mainstream capnometer

Diploma Master Thesis

Study program:	**Biomedical and Clinical Technology**
Study branch:	**Biomedical Engineering**
Diploma thesis supervisor:	**Assoc. prof. Ing. Petr Kudrna, Ph.D.**
Diploma thesis author:	**Bc. Ortiz Santiago, Victor**

Kladno 2022

MASTER'S THESIS ASSIGNMENT

I. PERSONAL AND STUDY DETAILS

Student's name:	**Ortiz Santiago Víctor**	Personal ID number:	**491393**
Faculty:	**Faculty of Biomedical Engineering**		
Department:	**Department of Biomedical Technology**		
Study program:	**Biomedical and Clinical Technology**		
Branch of study:	**Biomedical Engineering**		

II. MASTER'S THESIS DETAILS

Master's thesis title in English:

Design and development of mainstream capnometer

Master's thesis title in Czech:

Design and development of mainstream capnometer

Guidelines:

Design and implement a prototype of mainstream capnometer, usable in the neonatal breathing circuit sets at the mechanical ventilation. Design the capnometer as an open system with the possibility of further development. The basic requirement for tthe system is continual measurement of capnographic curves, analysis of etCO2 and transfer of measured data to a PC for further processing. Compare the implemented device with a commercially available device and evaluate the differences.

Bibliography / sources:

[1] John G. Webster, Encyclopedia of Medical Devices and Instrumentation, ed. 6, Wiley, 2006, ISBN 978-0-471-26358-6
[2] Tricia L. Gomella, Neonatology: management, procedures, on-call problems, diseases and drugs, ed. Sixth Edition, McGraw Hill Professional, 2009, ISBN 78-0-07-154431-3
[3] Walter Boron, Emile L. Boulpaep, Textbook of Medical Physiology, ed. 2nd, Elsevier, 2009, ISBN 978-1-4160-3115-4

Name of master's thesis supervisor:

doc. Ing. Petr Kudrna, Ph.D.

Name of master's thesis consultant:

doc. Ing. Martin Rožánek, Ph.D.

Date of master's thesis assignment: **15.02.2022**
Assignment valid until: **22.09.2023**

doc. Ing. Martin Rožánek, Ph.D.	prof. MUDr. Jozef Rosina, Ph.D., MBA
Head of department's signature	Dean's signature

DECLARATION

I hereby declare that I have completed this thesis having the topic “Design and development of mainstream capnometer” independently, and that I have attached an exhaustive list of citations of the employed sources.

I do not have a compelling reason against the use of the thesis within the meaning of Section 60 of the Act No.121 / 2000 Sb., on copyright, rights related to copyright and amending some laws (the Copyright Act).

In Kladno 12. 5. 2022 Bc. Victor Ortiz Santiago

ACKNOWLEDGEMENTS

I would like to express my gratitude and appreciation to the supervisor of this thesis Assoc. Prof. Ing. Petr Kudrna, Ph.D., whose guidance, patience and encouragement has been invaluable throughout this work. I am also thankful to the rest of my colleagues from the Faculty of Biomedical Engineering at Czech Technical University for giving me the opportunity to be part of this eminent institution. To conclude, I cannot forget to thank my family because without their unconditional support none of this would have been possible.

This thesis was supported by the student grant "Control systems for therapeutic medical devices in resuscitation and intensive care" from Czech Technical University (NºSGS22/204/OHK4/3T/17).

ABSTRACT

Design and development of mainstream capnometer

This thesis deals with the design and construction of a mainstream capnometer for the continuous measurement of carbon dioxide concentration in the patient´s respiratory circuit during mechanical ventilation, performed by an optical sensor using infrared absorption spectroscopy. The device was designed with technical focus on individual components needed for subsequent implementation as an open system, intended to be used in intubated neonates during high frequency ventilation. The data obtained from the sensor is processed externally using LabVIEW software, displaying the results as capnography curves with real-time changes of CO_2 concentration. The main goals were to verify the functionality of the final implemented device to measure changes in CO_2 concentration, create the characteristic calibration curve of the device from the results of the measurements and verify if it is usable in high frequency ventilation modes. For these purposes, static and dynamic tests were performed and the results were analysed and compared using a reference capnometer.

Key words

Capnography, CO_2 detector, infrared spectroscopy, mechanical ventilation, high frequency ventilation, end-tidal CO_2, signal analysis.

Table of Contents

List of symbols and abbreviations

Symbol/Abbreviation	Importance/meaning
$EtCO_2$	End tidal carbon dioxide
NDIR	Non-dispersive infrared absorption
ETT	Endo Tracheal Tube
ATP	Adenosine triphosphate
MV	Mechanical Ventilation
PIP	Peak Inspiratory Pressure
PEEP	Positive end-expiratory pressure
AARC	American Association for Respiratory Care
VILI	Ventilator Induced Lung Injury
ARDS	Acute Respiratory Distress Syndrome
COPD	Chronic Obstructive Pulmonary Disease
ECMO	Extra Corporeal Membrane Oxygenation
FRC	Functional Residual Capacity
HFV	High Frequency Ventilation
HFJV	High Frequency Jet Ventilation
HFOV	High Frequency Oscillatory Ventilation
HFPPV	High frequency positive pressure ventilation
HFPV	High frequency percussive ventilation
MAP	Mean airway pressure
ICU	Intensive Care Unit
Hz	Hertz
I:E	Inspiratory time to expiratory time ratio
IBW	Ideal Body Weight
ICU	Intensive Care Unit
MAP	Mean Arterial Pressure
PAP	Pulmonary Artery Pressure
PEEP	Positive End-expiratory Pressure
PIP	Peak Inspiratory Pressure
ETT	Endotracheal Tube
ppm	Parts per Million
DAQ	Data Acquisition
VI	Virtual Instrument
Lpm	Litres per minute
$\dot{V}/\dot{Q}$	Ventilation/perfusion ratio
FFT	Fast Fourier Transform
bpm	Breaths per minute
bps	Breaths per second

1 Introduction

Nowadays mechanical ventilation has become one of the most crucial tools of the health care systems all over the world, especially in intensive care units as life support for critical patients because it can increase their chances of survival. Moreover, demand for it since the covid-19 pandemic has rocketed [1]. But if mechanical ventilation is not performed and controlled properly, there can be fatal consequences for the patient [2]. For this reason, devices like capnometers and pulse oximeters are fundamental because they can monitor parameters related to respiratory processes. Blood gas analysis is another very used and precise method, however it is invasive. In the case of new-borns, the use of non-invasive techniques is more indicated because of limited blood volume avoiding the risk of bleeding and further complications. Therefore, oximetry and capnography are the main non-invasive methods used as indicators of the actual state of the vital functions of new-borns [3]. There are many different physiological parameters that can be measured. However, there are strong arguments to suggest that the measure of carbon dioxide concentration from the breathing air is one of the most valuable parameters that can be obtained during mechanical ventilation, because it provides a wide range of information about the state of the patient that would probably be missed if other parameters were used. The level of CO_2 in the body is helpful to detect and evaluate different problems. For example in the pulmonary circulation, it reflects changes sooner than oximetry and find if there is airway obstruction, how the ventilation or cardiopulmonary resuscitation is working, verify if the intubation was done properly etc… [4]. Therefore, CO_2 monitoring plays an important role and can be crucial for the patients as well as being non-invasive, simple and relatively inexpensive tool to use. Capnography is already a standard tool used to monitor mechanically ventilated patients. However, it is important to consider the physiological and technical limitations in neonates due to the differences in the lungs and breathing patterns between neonates and adults [5]. These differences may alter CO_2 measurements as well as the interpretation of the capnograms and derived parameters. The high respiratory rate and low tidal volume in new-borns, especially during high frequency ventilation, require mainstream sensors with extremely quick response to avoid misleading measurements. Moreover, there is a lack of capnometers on the market designed for high frequency ventilation which is a widely used ventilation mode in neonates. All these facts represent the main reason and technical challenge for this thesis.

2 Overview of the current state of the art

This chapter deals with the importance of the carbon dioxide for the human body, how it is produced, transported, eliminated, measured and monitored from the patient breathing circuit. Most commonly used methods and technologies are also explained next.

2.1 Carbon dioxide in the human body

Carbon dioxide is a colourless, odourless, incombustible gas resulting from the oxidation of carbon. It is also a metabolic waste product produced by cellular respiration from the ingested nutrients in form of glucose and oxygen to provide energy in the form of adenosine triphosphate (ATP) following the next reaction:

$$C_6H_{12}O_6 + 6O_2 \rightarrow 6CO_2 + 6H_2O \quad (1)$$

After being produced, carbon dioxide is transported from the cells to the bloodstream by diffusion. Then, by circulatory transport, it reaches the lungs where from the pulmonary capillaries diffuses through the alveolar membrane into the alveoli and is removed from the body through exhalation to the environment. The driving force for CO_2 diffusion is the difference in the partial pressure of CO_2 between the alveolar space (about 40 mmHg) and the blood in the pulmonary capillary (about 46 mmHg). Even though the difference is small, CO_2 exchange is ensured because of its excellent solubility, which is higher than that of oxygen. CO_2 mainly dissolves in water to produce carbonic acid (H_2CO_3), which, in turn, converts into bicarbonate (HCO_3^-) and hydrogen ions (H^+) under the following reaction [6]:

$$CO_2 + H_2O \leftrightarrow H_2CO_3 \leftrightarrow H^+ + HCO^-_3 \quad (2)$$

If CO_2 levels are maintained outside of the physiological range, it can cause hypo or hypercapnia, both serious conditions that can result in cell, tissue, and organ damage as well as death [7]. The CO_2 concentration is usually measured in parts per million or ppm (1 % = 10000 ppm). Approximately, the concentration of CO_2 in the air is 0,04 % by volume (from 400 to 600 ppms is the normal outdoor range) and it goes up from ~ 3,8 % to 5,0 % during exhalation. 5000 ppm is considered the maximum safe level concentration without health risks.

Carbon dioxide plays an essential role in the human body including regulation of blood pH, respiratory drive, and affinity of haemoglobin for oxygen...etc. If the carbon dioxide level in the body is not properly regulated and controlled, it can cause different health problems if abnormal levels are maintained [8]. For these reasons, CO_2 monitoring or capnography has become a standard and essential method especially during mechanical ventilation. It was first time used during World War II as a tool for monitoring the internal environment and after introduced in to medical use in 1950 to measure the amount of exhaled CO_2 during anaesthesia but it was not used in the clinical practice till 1980 decade with the development of more effective devices [9].

2.2 Measurement of carbon dioxide concentration

There are many different methods for the measurement of CO_2 that can be used. They can be mainly electrochemical, electroacoustic, colorimetric, conductive and optical methods. However, optical methods had proven to be the most sensitive and accurate ones besides being non-invasive, which is a great advantage for neonates. The mechanism of action most widely used in optical methods to determine the amount of CO_2 is called infrared spectroscopy, which is the study of interaction of electromagnetic waves with matter within the infrared spectrum, also known as non-dispersive infrared absorption (NDIR). Often IR radiation is considered as thermal radiation. By 1900 IR spectroscopy became an important tool for identification and characterization of chemical compounds and materials since their IR spectrum is the "fingerprint" of the substance [10]. This method is based on the on the Beer–Lambert law:

$$I = I_0 \cdot e^{-\alpha CL} \tag{3}$$

Where I is the intensity of light striking the detector (W/cm^2), I_0 is the measured intensity of an empty sample chamber (W/cm^2), α is the absorption coefficient (cm^2/mol), C is the CO_2 concentration (mol/cm^3) and L is the absorption path length (cm) [11].

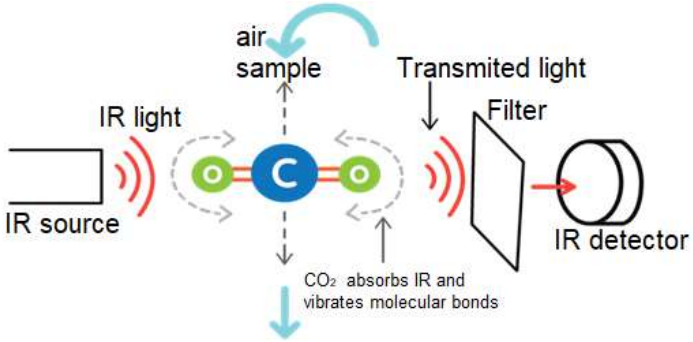

Figure 2.1: Non-Dispersive Infrared Absorption diagram [12]

As shown in the Figure 2.1, when CO_2 molecules are exposed to light with specifics wavelength, the molecule will absorb a specific amount of that light, and according to Beer–Lambert law, the absorption of the light is proportional to the CO_2 concentration that can be calculated. Carbon dioxide presents specific peaks of absorption on the infrared radiation (IR) spectrum in three narrow bands of wavelengths, which are 2.7, 4.3 and 15 micrometres. So this method of analysis can be considered both quantitative (how much substance) and qualitative (which substance). However, there are different substances present in the air such as nitrogen, nitrous oxide and oxygen, so the measured absorption of CO_2 can be altered by cross interference and collision broadening. For this reason the use of narrow band sources or narrow band filters can effectively eliminate this effect [13]. This is a very important aspect to consider for the selection of the appropriated components for the capnometer to perform the most accurate measurement. NDIR gas sensors have proven to have good stability, high selectivity and fast response. In recent years, the development of NDIR CO_2 sensors has made a great progress.

There are two different ways employed to obtain the signal that represent the correlation between the intensity of the IR light and the values of CO_2 concentration. It can be done with or without moving parts, which is also called not solid and solid state sensors respectively. Solid state sensors use a beam splitter to simultaneously measure the IR light at two wavelengths: one which is absorbed by CO_2 (data) and one which is not (reference). Also, the IR light source can be electronically pulsed. NDIR CO_2 sensors which are not solid state employ a spinning disk known as a chopper wheel, which can periodically interrupt the IR beam at a given frequency, which will be the sampling frequency [14].

2.2.1 Factors influencing infrared measurements:

- Atmospheric pressure: the increased pressure directly affects the number of CO_2 molecules absorbing the IR energy, but changes in atmospheric pressure caused by the change in weather do not significant effect on signal change.

- Nitrogen dioxide: has the ability to absorb IR radiation at wavelengths between 4,5 and 6,5 μm, thus a narrowband IR filter is required for its elimination.

- Oxygen: although it is not absorbing IR radiation, it may indirectly affect CO_2 absorption due to collisions that cause falsely low CO_2 values.

- Water vapour: due to condensation on the sensor window, it can cause the absorption of IR radiation, leading to higher measured CO_2 values than they actually are. Elimination is possible by heating the sensor above body temperature or eliminating the excess water vapour.

- Inhalation agents (under anaesthesia): do not have a very significant effect on IR absorption radiation because they have different IR absorption spectrum than CO_2 as shown in Figure 2.2.

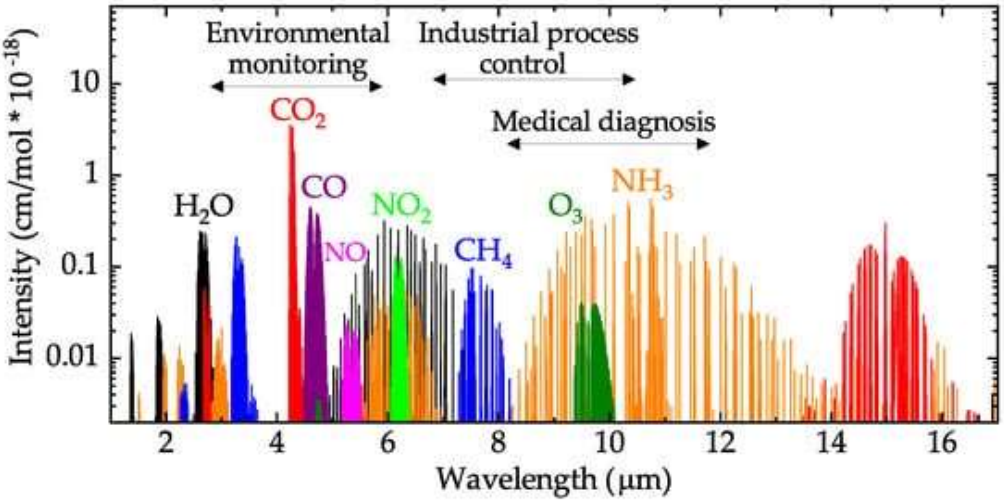

Figure 2.2: Mid-infrared absorption spectra of different molecules with their relative intensities [15]

The main structural elements of the designed CO_2 detector are described next, which can be divided into next parts: IR source, IR detector and the airway adapter.

2.2.2 IR radiation sources

Infrared or thermal radiation, is the band in the electromagnetic radiation spectrum with wavelengths above red visible light between 780 nm and 1 mm and it is divided into three regions: the near-infrared (0,78–3,00 μm), mid-infrared (3–50 μm) and far- infrared (50–1000 μm), named according to their distance to the visible spectrum. The source of radiation can be divided generally into natural (sun or fire) and artificial (heating devices, IR lamps, lasers…) or it can be also classified as incandescent (emission of radiation due to the high temperature of an object) or luminescent sources (photons are emitted without heat being the cause). Actually, any substance above absolute zero temperature emits infrared radiation.

2.2.3 IR radiation detector: Thermopile

A thermopile is an electronic device that generates electric voltage from thermal or infrared radiation due to the thermoelectric effect. It is composed by a group of thermocouples connected in series. Each thermocouple consist of two dissimilar metals connected forming an electrical junction, when the junction of the two metals is heated, a temperature gradient is created in the circuit thus, a small voltage is generated which is proportional to the temperature difference as shown in Figure 2.3.

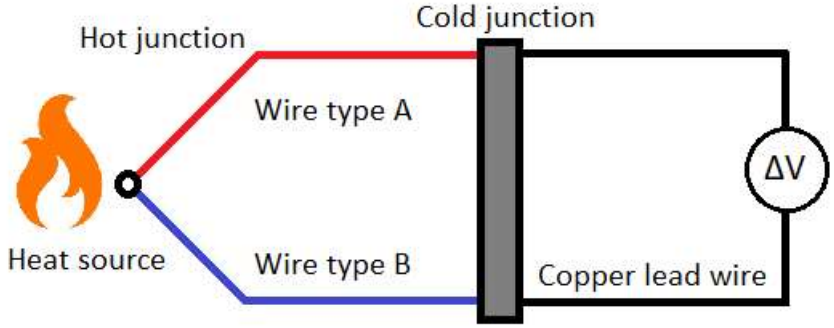

Figure 2.3: Thermocouple diagram

A thermopile with N thermocouples will output a voltage N times bigger than the one produced by a single thermocouple, increasing the sensitivity of the transducer. Main advantages are that external power supply is not needed, the stable response characteristics of the sensor, it is simple, robust and cost-effective temperature sensor used in a wide range of applications. Concentration of various types of gases can be measured by attaching a band-pass filter to thermopile detectors. The most common gases that are measured with the NDIR principle are carbon dioxide, carbon monoxide, nitrogen oxide, methane and hydrocarbons. This type of detector normally uses an optical filter to eliminate all the unwanted wavelengths except the one that the selected gas molecules can absorb.

2.3 CO_2 Monitoring clinical meaning

End-tidal carbon dioxide ($EtCO_2$) is the maximum level or concentration value of carbon dioxide during a breathing cycle and it is measured at the end of the exhalation. This value is very important because it reflects how the carbon dioxide is being eliminated from the body and it can provide an indication of cardiac output and pulmonary blood flow. Sudden changes in $EtCO_2$ pressure quickly reflect circulatory and/or ventilatory compromise [16].

Non-invasive methods for CO_2 monitoring include capnometry and capnography. While capnometry refers to the numerical display of end-tidal CO_2 value for each breath, capnography is the graphical representation of the partial pressure of CO_2 along the breathing cycle, and it can be expressed as partial pressure, mmHg, concentration, fractions or percentages. Capnography allows real time monitoring of the patient ventilation status and the identification of potential breathing complications (such as airway obstruction, hyperventilation, hypoventilation, apnea, verify correct intubation…) and respond accordingly with a change in clinical management (for example, providing supplemental oxygen or reassessing the patient) [17]. This technique can be used in both intubated and non-intubated adults and neonates under mechanical ventilation [18]. According to the American Association for Respiratory Care (AARC) Clinical Practice Guideline for Capnography/Capnometry During Mechanical Ventilation [19], during capnography the following parameters should be also considered and monitored:

- Ventilator variables: tidal volume, respiratory rate, positive end-expiratory pressure, ratio of inspiratory-to-expiratory time, peak airway pressure, and concentrations of respiratory gas mixture.
- Hemodynamic variables: systemic and pulmonary blood pressure, cardiac output, shunt, and $\dot{V}/\dot{Q}$ (ventilation/perfusion ratio) imbalances.

The output waveform of the capnometer can be plotted over time or sampled volume:

- Conventional or time-based CO_2 monitoring is widely used and represents the elimination of CO_2 concentration over time, it is a simple method however there is some risk of misleading measurements in case of inaccuracy and therefore poor estimation about the ventilation and perfusion of the patient.
- On the other hand, volumetric CO_2 monitoring represents the expired CO_2 over the expired tidal volume (instead of time) and is suggested to assess CO_2 elimination and the ratio of dead-space volume to optimize mechanical ventilation [19].

However, the implementation of volumetric capnography is harder because it requires to measure not only the CO_2 but also the tidal volumes by flow sensors, which could be very complicated and expensive task in some cases, especially in new-borns where the tidal volumes are really small and even smaller when high frequency ventilation is used (< 1 ml) [20]. For this reason, was decided that the most appropriated method for this project was the use of time-based capnography instead of volumetric capnography.

2.4 Mainstream, sidestream and microstream capnography

There are two main different configurations for the use of capnography (Figure 2.4). It can be sidestream (first generation) and mainstream (second generation). The main difference between both, is basically the location of the CO_2 sensor: while in mainstream the sensor is located directly between the endotracheal tube and the breathing circuit, sidestream capnography transports a portion of a patient's respired gases from the sampling site, through a sampling tube to the sensor, which causes a time delay on the reading [11].

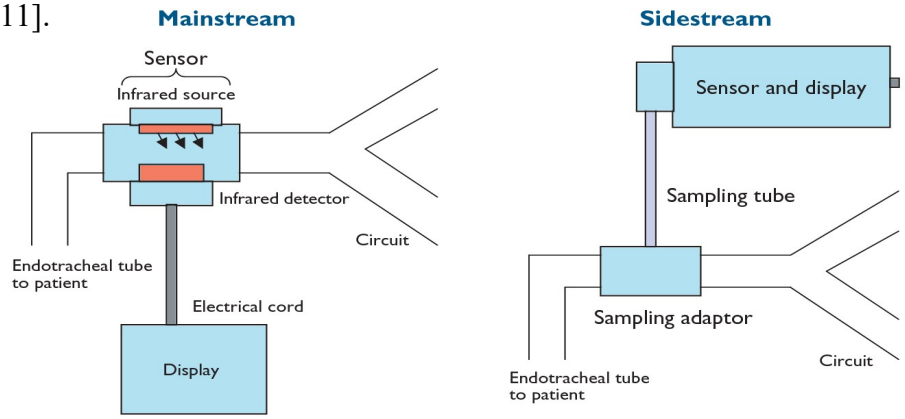

Figure 2.4: Mainstream and sidestream configuration diagram [21]

As an advantage for both technologies, they have been integrated in the last decades into mechanical ventilators, so the CO_2 values are displayed on the ventilator monitor, this is extensively used in intensive care units. The main advantage of mainstream over sidestream technology is, as mentioned before, that mainstream capnography does not present any delay in the measurement, so the values displayed in the monitor are real-time values, while in sidestream capnography, as the sample goes through the sampling tube to the external sensor, there is a delay on the reading that can be up to two seconds or even more. One advantage of sidestream capnography over mainstream, is that the airway adapter is lighter because it does not have the sensor on it. This is an important aspect for neonates because it makes it more applicable. Mainstream capnography can be heated using a wire to avoid condensation and line occlusion so is less prone to error than sidestream capnography, however it requires more frequent calibration [22].

On the other hand, there is one more recent technique called microstream capnography, based on molecular correlation spectroscopy. It uses a highly CO_2 specific infrared source where the IR emission precisely matches the absorption spectrum of the CO_2 molecules, eliminating interferences from other gases and allowing sample cells with much smaller volumes (15 µml) that permit low flow rates (50 ml/min) with high accuracy. The sampling circuit is also designed to provide oxygen at the same time while using a hydrophobic filter reducing the risk of occlusion. However, its implementations is much harder and as it is a relative new technique there is a lack of relevant literature regarding microstream, for these reasons it was discarded for this project.

The Table 2.1 shows a summary with the main pros and cons for each configuration.

Table 2.1: Advantages and disadvantages of main/side/microstream capnography

	MAINSTREAM	***SIDESTREAM***	***MICROSTREAM***
ADVANTAGES	Easily integrated with the ETT	Allows monitoring of non-intubated subjects	Highly efficient and selective
	No time delay	Lighter airway adapter	Really small samples (15 µl)
	Can be heated	Less calibration needed	Can provide oxygenation and ventilation
	Less prone to error	Uses filter/water trap	No calibration required
DISADVANTAGES	Heavier airway adapter	No heat: condensation, line occlusion…	Harder implementation
	Requires more frequent calibration	Time delay (up to 2 s)	Expensive
	Possible risk of burns	Less accurate in neonates (larger sample volume)	Lack of literature available

2.5 Capnograms and waveform analysis

A capnogram (Figure 2.5) is a waveform of the CO_2 concentration during respiration and is an extremely valuable clinical tool that can be used for many applications especially during mechanical ventilation, where it has three main roles: to support the proper ventilation of the patient, detect problems with the mechanical ventilation circuit and verify correct intubation [23]. Normal $EtCO_2$ values are 30 - 43 mmHg.

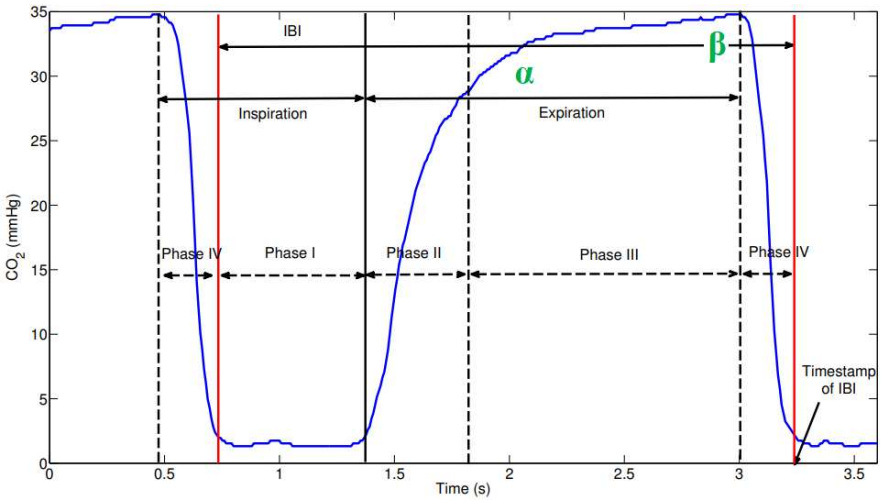

Figure 2.5: Normal time-based capnogram and its different phases [24]

A normal capnogram (Figure 2.5) is the standard waveform of a healthy patient and it presents four differentiated phases:

- Phase I or A-B: also called baseline and represents the end of inhalation and beginning of exhalation (dead space ventilation). Here the concentration of CO_2 should be very close to 0 (in the air is 0,04 %).

- Phase II or B-C: (or expiratory upstroke) a very fast increase of CO_2 is observed at the beginning of exhalation by the elimination of CO_2 of the dead space mixed with alveolar CO_2.

- Phase III or C-D: expiratory alveolar plateau. The exhalation of the CO_2 from the alveoli takes place. It reaches the peak ($EtCO_2$) where the partial pressure of CO_2 is the highest.

- Phase IV or D-E: at the beginning of the inspiration the partial pressure of CO_2 decreases rapidly from the maximum value to almost 0 at the end of the inspiration [25].

By analysing the shape of the obtained capnogram from the patients is possible to find out how is their physiological status. Different pathologies show specific changes or patterns in the capnogram that distinguish and allow to identify them [26]. Most common parameters that are measured from the capnograms are the angles (alpha ≈ 110º and beta ≈ 90º to 110º), slopes, peaks of expiratory and inspiratory CO_2 values and relative duration of each phase [27].

2.5.1 Abnormal capnograms and interpretation

Healthy individuals will present capnograms with similar rectangular shape as shown before, but any changes on them requires adequate analysis and interpretation to determine the possible causes. These changes are usually the earliest indication of ventilatory problems and their correct interpretation can reduce errors in diagnose or clinical interventions. Moreover, diseases, anaesthesia, and surgery can affect the transition from intrauterine to extra uterine life in the case of new-borns altering their capnograms too. Nowadays several factors have contributed to improved survival in neonatal surgery as increased understanding of neonatal physiology, advances in airway management, monitoring and the establishment of neonatal intensive care units [28].

Figure 2.6 summarizes the most relevant waveform patterns that can be found during capnography and their clinical interpretation with other possible causes for that specific shape:

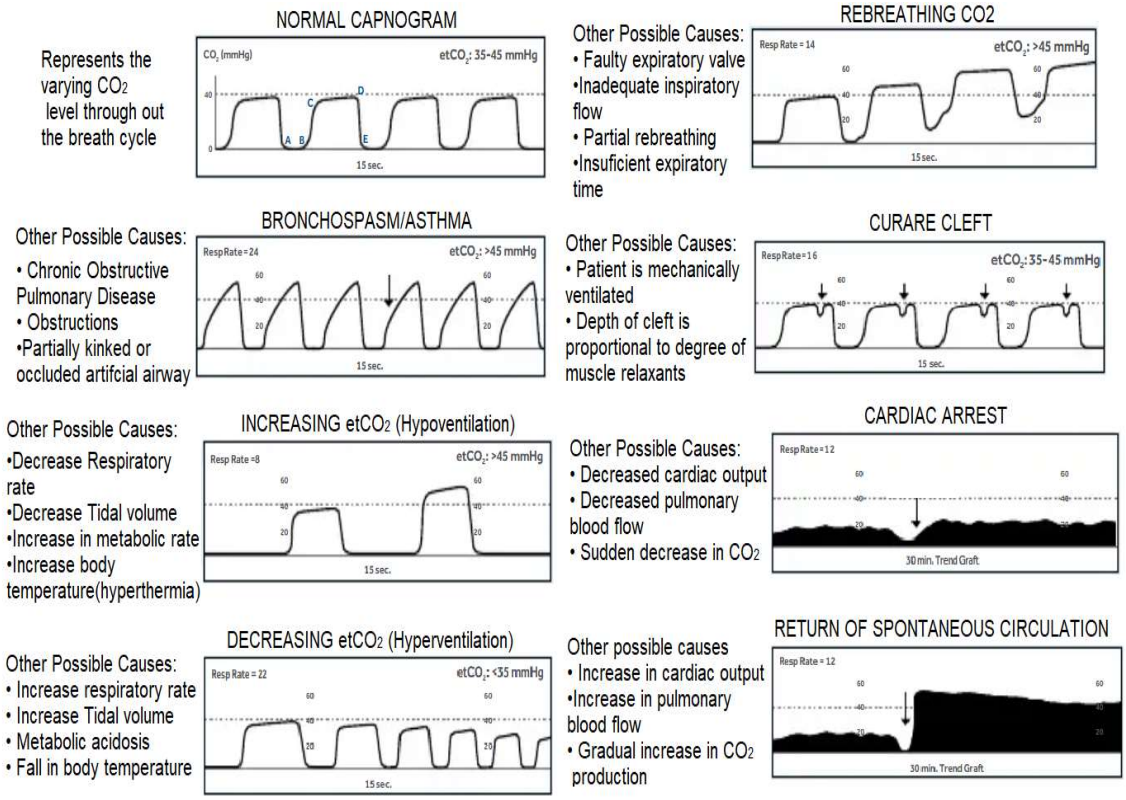

Figure 2.6: Most Relevant capnography waveforms and their interpretation. Modified from source [29]

2.5.2 Trend functions

Monitoring trend functions of CO_2 allows more comprehensive analysis of the patient condition and detection of early sign of many related diseases such as pulmonary emboli, chronic obstructive pulmonary disease, acute respiratory distress syndrome, etc. As it is observed in the black-marked capnograms in Figure 5, the CO_2 changes are recorded for 30 minutes instead of the 15 seconds of the rest of them.

However, some studies show that paediatric patients do not tolerate wearing capnography cannula for prolonged periods of time, limiting the usefulness of it as a continuous monitor of mechanical ventilation until more effective, child-friendly devices are developed and their utility validated. For these and other reasons, guidelines recommended for adult patients cannot be extended to children [30].

2.6 Mechanical ventilation

Mechanical ventilation (MV) can be defined as the technique through which gas is moved toward and from the lungs through an external device connected directly to the patient [31]. As mentioned before, mechanical ventilation can be a lifesaving intervention in critically ill neonates aiming to achieve adequate gas exchange in the lungs, to reduce respiratory effort, to obtain lung expansion, to allow sedation, etc... However, it also has the potential to cause significant damage to the lungs resulting in long-term complications. Minimize ventilation-induced lung injury (VILI) should be considered by choosing the appropriate modes and settings of ventilation [32]. The major indication for mechanical ventilation is acute respiratory failure and its main goals are relieve respiratory distress, decrease work of breathing, improve pulmonary gas exchange, reverse respiratory muscle fatigue…Permitting lung healing and avoiding further complications [33].

The main modalities of conventional ventilation (CV) are pressure targeted, volume targeted, and hybrid ventilation. When using pressure-controlled (PC) ventilation, the ventilator delivers a flow of gas until the pressure (called peak inspiratory pressure or PIP) set by the operator is delivered to the patient. Positive End Expiratory Pressure (PEEP), which is the remaining pressure in the lungs at the end of an expiration, can also be set. Similarly, in the volume-controlled (VC) ventilation, the ventilator delivers the volume set by the operator as it is shown in Figure 2.7.

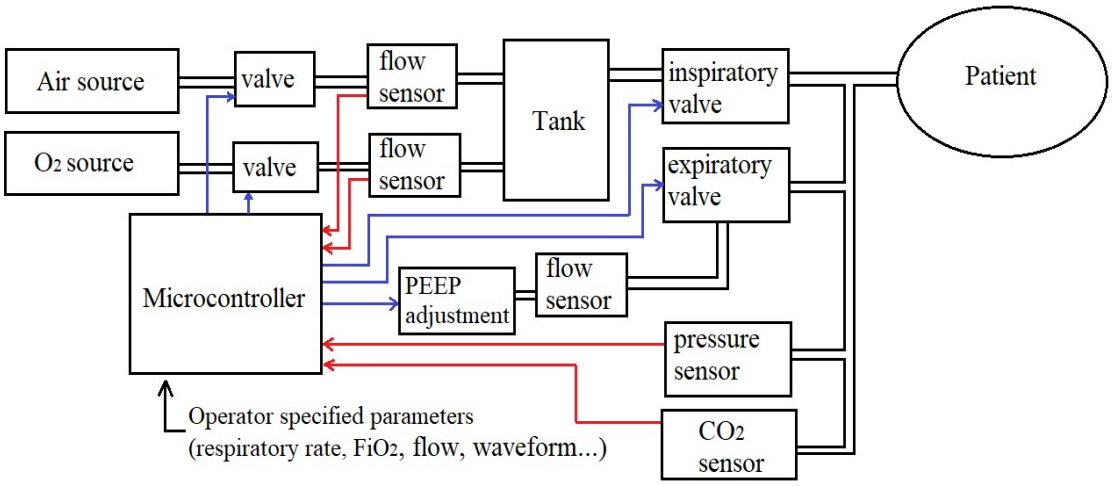

Figure 2.7: Block diagram of a basic mechanical respiratory ventilator

The initial settings of the tidal volume depends on the lung status:

- Normal = 12 mL/kg ideal body weight (IBW).
- Chronic Obstructive Pulmonary Disease (COPD) = 10 mL/kg IBW.
- Acute Respiratory Distress Syndrome (ARDS) = 6 - 8 mL/kg IBW.
- The normal respiratory rate is between 10 and 12 breaths per minute.

There are many other modes to perform mechanical ventilation, some of the most relevant are mentioned next:

- Controlled Mechanical Ventilation: the ventilator delivers a present number of breathes/min of a pre-set volume. Additional breathes cannot be triggered by the patient, as in the case of ACV. It is used in patients who are paralyzed.

- Assist Control Ventilation: delivers a pre-set volume when patient triggers the machine automatically if patient fails to trigger within selected time. Clinician sets tidal volume, back-up rate, sensitivity, flow rate.

- Intermittent Mandatory Ventilation: delivers a pre-set volume at a pre-set rate. Permits spontaneous breathing (unlike assisted control ventilation).

-Nonconventional Mechanical Ventilation modes: such as non-invasive nasal ventilation, high frequency ventilation, pulmonary gas exchange devices (ECMO, $ECCO_2$ removal), constant flow ventilation, and etc.

2.6.1 High frequency ventilation

High frequency modes for mechanical ventilation were developed in response to problems associated with conventional ventilation. On the contrary to CV, HFV do not try to replicate normal breathing. It provides ventilation using much smaller tidal volumes (it can be even smaller than the dead space) delivered at rates 10 times higher than normal. It has been proven by many clinical studies that smaller tidal volumes cause less lung injury, being this aspect the key for this ventilation strategy. High frequency modes are an essential tool in supporting premature infants because it reduces the risks and helps prevent ventilator-induced lung injury [34]. It also maintains constant alveolar inflation and thus prevents the inflating-deflating cycle and therefore improves oxygenation too.

There are mainly four types of HFV [35]:

- High frequency oscillatory ventilation (HFOV)
- High frequency positive pressure ventilation (HFPPV)
- High frequency jet ventilation (HFJV)
- High frequency percussive ventilation (HFPV)

Indications for high frequency ventilation (HFV) in neonates include [36]:

- Persistent pulmonary hypertension (lung vessels are not open wide enough meaning that oxygen and blood flow is restricted)
- Acute respiratory distress syndrome (ARDS)
- Pulmonary interstitial emphysema (air gets trapped outside of alveoli)
- Meconium aspiration (meconium/amniotic fluid in the lungs)
- Pulmonary hypoplasia (incomplete development of lungs)

2.6.2 High Frequency Oscillatory Ventilation

In patients with failing conventional ventilatory therapy, alternative ventilatory modes such as high frequency oscillatory ventilation (HFOV) can be beneficial. As mentioned before, in this mode of ventilation tidal volumes are extremely small, and ventilatory frequency is high (3 – 15 Hz). Furthermore, a continuous flow of fresh gas, or bias flow, is used to maintain a stable relatively high airway pressure (PEEP). When the respiratory system is inflated to the point where its compliance is highest, tidal volume and ventilation will be maximal with CO_2 clearance. Energetically, this is an optimal breathing strategy for infants with stiff lungs, as it reduces the work of breathing. HFOV can provide the highest mean airway pressure paired with the lowest tidal volume of any mode [37]. These benefits make HFOV the ideal lung-protective ventilation strategy and the most currently used between HFV modes. However, this breathing strategy results in a technical challenge in capnography measurements using currently available equipment.

There are several reasons to apply HFOV on new-borns, some of the most relevant are mentioned next. Table 2.2 shows the main indications and hazards of HFOV.

- Easy transmission of the mean airway pressure
- Open the lung at lower pressure (maximizes alveolar recruitment, improves oxygenation)
- Lower pressure gradient needed
- Higher frequency can be used
- Can prevent from injuries

Table 2.2: Indications, contraindications, and hazards associated with the use of HFOV [38]

INDICATIONS	CONTRAINDICATIONS/HAZARDS
Ventilator-associated lung injury	Higher intrathoracic pressures
Alveolar haemorrhage	Pneumothorax
Large air leak with inability to keep lungs open	Migration/displacement of ETT
Failure of conventional mechanical ventilation	Bronchospasm
Refractory hypoxemia	Airway obstructions
Abdominal Compartment Syndrome	Barotrauma
Increased intracranial pressure	Sepsis
Persistent pulmonary hypertension	Subcutaneous emphysema
Acute Respiratory Distress Syndrome	Multiple organ failure
Pulmonary Interstitial Emphysema	Refractory acidosis
Meconium aspiration	Intraventricular haemorrhage
Pulmonary hypoplasia	Cellular injury
Broncho pulmonary fistulae	High pulmonary capillary wedge pressure

The device called oscillator, delivers a constant flow of heated, humidified gas, providing flow rates (bias flow) of 20 to 60 Lpm. This flow produces a constant mean airway pressure (MAP). An oscillating piston pump then vibrates the pressurized gas at a frequency that is generally set between 3 and 15 Hz (180 – 900 cycles/min) as it is observed in the Figure 2.8. As the membrane moves forward and backward, some of the flow is pushed in and out of the lungs. The power setting (amplitude) on the ventilator controls the distance and velocity (frequency) that the membrane moves from its resting position. This oscillatory pressure amplitude, or delta P (ΔP), is set to achieve desired CO_2 elimination. In HFOV, both expiration and inspiration are active processes, and a single ventilator provides both ventilation and oxygenation to patients.

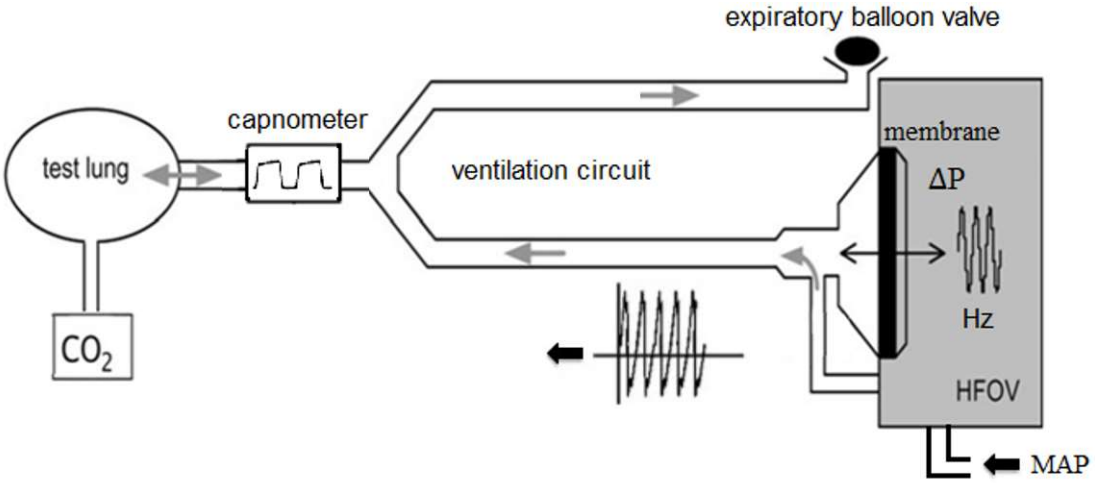

Figure 2.8: Basic diagram of HFOV system. Modified from source [39]

2.6.3 High Frequency Jet Ventilation

High frequency jet ventilation (HFJV) is significantly different from HFOV. Both are extensively used modes in neonates and children with severe respiratory failure [40] but in HFJV, a pneumatic valve releases short jets of gas in the inspiratory circuit, and expiration is passive. HFJV rate is usually set based on the patient's size and disease state, with neonates usually initiated at 420 breaths/min. In the paediatric ICU, the rate is usually started between 360 – 420 breaths/min. It is used in conjunction with conventional mechanical ventilation, with application of PEEP. During HFJV, it is possible to combine fast and low-volume inspirations with relatively long expirations and an inspiratory-expiratory ratio as low as 1:12 [41].

The main advantage of HFJV is minimised lung trauma by using ultra-low tidal volumes, minimising also the level of required supplemental oxygen that could be harmful for neonates. One advantage over HFOV is that spontaneous breathing is more easily achieved in parallel with HFJV and may be more comfortable for the infant as end-expiratory pressure is lower than during HFOV. This also potentially allows better lung perfusion than during HFOV due to lower pulmonary vascular resistance [42].

Main complications associated with HFJV:

- ETT Obstruction (same as CV).
- Tracheal Injury (same as CV).
- Hypercarbia due to inadequate tidal volume consequent to inadequate HFJV amplitude, insufficient inspiratory time or inadequate HFJV rate.
- Hypocarbia resulting from excessive tidal volume due to excessive HFJV amplitude, excessive inspiratory time or excessively high HFJV rate.
- Hyperinflation and/or inadvertent PEEP (air trapping) and potential development of air leak syndrome (pneumothorax, pulmonary interstitial emphysema) due to inappropriately high ventilator rate or excessive PEEP (hyper-inflation without gas trapping).
- Atelectasis with risk of hypoventilation and lung injury due to inadequate PEEP.

As observed in Figure 2.9, a conventional ventilator is always used in parallel with the jet ventilator. It provides gas for the patient's spontaneous breathing, and it delivers occasional "sigh" breaths to recruit collapsed alveoli.

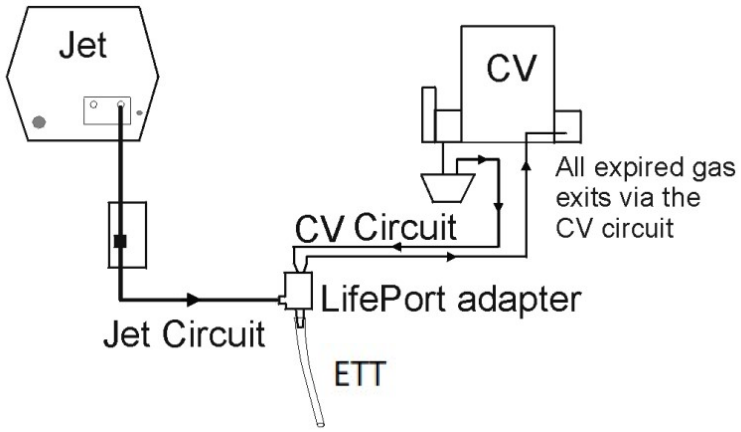

Figure 2.9: Basic diagram of HFJV system. [42]

Table 2.3 resumes the repiratory and frequency ranges associated with each ventilation mode related to this project.

Table 2.3: Ventilation modes with their frequency and respiratory ranges

Ventilation Mode	Respiratory Rate range (bpm)	Frequency range (Hz)
Conventional	10 to 20	0,16 to 0,33
HFJV	240 to 420	4 to 7
HFOV	180 to 900	3 to 15

In Figure 2.10, there is a graph comparing the different waveforms of these modes (CV, HFOV and HFJV), the average airway pressure of each technique is also marked (Paw). It is observed that for only one wave of the conventional ventilation mode there are several number of waves from the other modes at the same time:

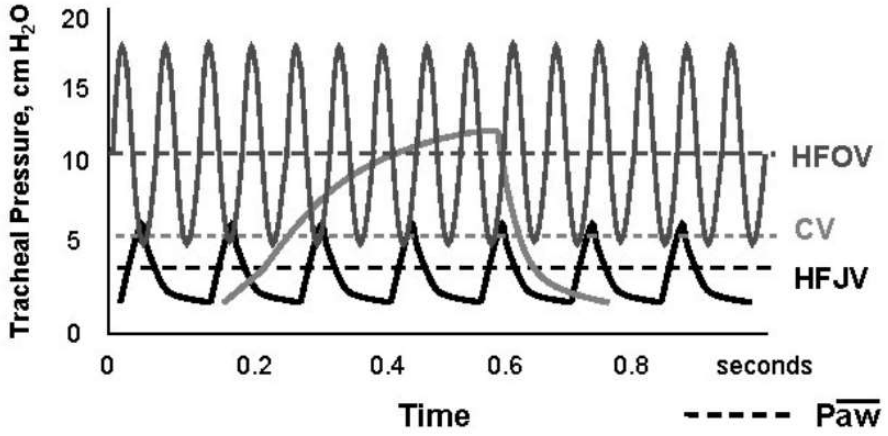

Figure 2.10: Pressure waveform comparison between HFOV, HFJV and CV [44]

2.7 Differences between adults and new-borns influencing CO_2 monitoring

Paediatric patients cannot be considered just as small adults. This fact is particularly true when considering the respiratory tract. Indeed, all organs experience a continuous process of maturation and development before and after birth, with consequent modifications in their dimensions, structure, physiology, location, and neurological control. Take into consideration the peculiarities of the paediatric airways is essential in the prevention, management, and treatment of acute and chronic paediatric respiratory diseases, especially in cases of life-threatening events [45], such as respiratory failure where CO_2 plays a crucial role.

The range of measurements for the CO_2 fraction (FCO_2) or the corresponding partial pressure (PCO_2) in the breathing gas is identical in neonates and adults. However, CO_2 production is much lower in neonates (from 9 to 15 mL/min) than in adults (about 200 mL/min) and in the field of neonatology, it is a challenge to measure $EtCO_2$ especially during high frequency ventilation because all the components are much smaller than in adults. For example the airflow, and therefore the dead space has greater impact than in adults and needs to be optimized. The much lower amount of exhaled CO_2 makes capnography in neonates much more difficult with the current methods and technical limitations of capnography in neonates.

Table 2.3 shows the main physiological differences in the implicated domains between children and adults. The differences and their causes/effects are compared and explained next.

Table 2.3: Differences in Respiratory physiology of the adult and the neonate

Domain	Neonate	Adult
Airways	Small mandible Large tongue Larger tonsils and adenoids Superior laryngeal position Soft, narrow, short trachea	Bigger size
Airway resistance	Respiratory resistance is increased at birth: bronchi are smaller and lung volumes are smaller	Lower airway resistance
Lung volumes and spirometer variables	FRC is similar to adult VT is similar to adult Minute volume is increased Respiratory rate is increased ERV is reduced Closing capacity is increased Anatomical dead space is increased (3,0 ml/kg)	Normal anatomical dead space is 2,2 ml/kg
Compliance	Lung compliance is decreased (less surfactant) Chest wall compliance is increased (cartilaginous ribs)	Good lung compliance Low chest wall compliance
Gas exchange	Increased shunt Oxygen toxicity includes retinopathy High oxygen-carrying capacity of blood	Normally shunt should be minimal Oxygen is relatively nontoxic
Control of respiration	Immature respiratory centre, Decreased response to hypercapnia Periodic apnoea and cyclical oscillating respiratory rate	Mature reflexes and rhythmogenesis
Respiratory energetics	The total oxygen consumption of the neonate is increased (6-10 ml/kg/min) Work of breathing is increased Ideal efficiency is at a respiratory rate between 30 and 50 Diaphragm is more susceptible to fatigue	Oxygen consumption is 3 ml/kg/min Max efficiency at respiratory rate 12-14

- Respecting the airways in neonates they are basically much smaller, making intubation much difficult in them.
- Respiratory resistance is higher at birth due to the presence of residual fluid in the lungs.
- In the neonate the dead space is also higher and therefore more tidal volume is wasted.
- Minute volume is bigger too in neonates due to a higher respiratory rate.
- Lung compliance is decreased usually due to an insufficiency of surfactant.
- In neonates the chest wall is three times more compliant than the lungs due to their cartilaginous ribs.
- Typically neonates present higher capacity of carrying oxygen in the blood because of increased haemoglobin. But the total oxygen consumption of the neonate is increased too. This means an increased metabolic rate and CO_2 production.
- The neonate's diaphragm is easier to fatigue, which has to be considered when respiratory failure occurs and during mechanical ventilation.
- As a result, the work of breathing is increased in neonates due to their increase in resistance and compliance, it takes more effort to produce breaths, and the more and deeper breaths, the greater the effort. It is critical to ensure that the tidal volume is low enough and the respiratory rate is high enough for the maximum efficiency.
- The most efficient respiratory rate in adults is between 12 and 14 while in neonates is between 30 and 50 breaths per minute.
- The ratio of tidal volume to body weight of neonates is between 6 and 7 mL/kg, almost the same as in adults, but it is slightly lower in preterm infants with 5 – 6 mL/kg. While vital capacity is double in adults than in neonates as observed on Figure 2.11.

Volume	Adult (ml/kg)	Neonate (ml/kg)
Tidal volume	6	6
Total lung capacity	86	63
FRC	34	30
Vital capacity	70	35
Residual volume	16	23
Closing capacity	23	35

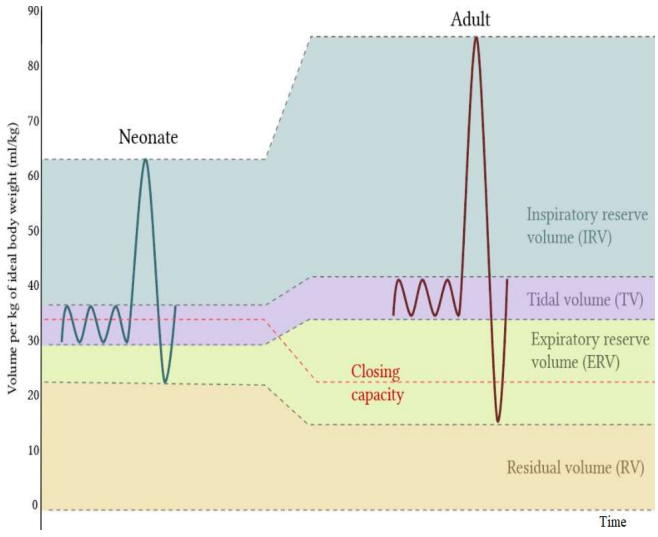

Figure 2.11: Volumes in adults and neonates, table and graph [46]

3 Aims

The main goal of this thesis was to design and implement a mainstream capnometer, which performs accurate and real time measurements of the carbon dioxide concentration changes present in the patient breathing circuit when mechanical ventilation is being used. More specifically, the device is intended to be used with new-born patients during high frequency mechanical ventilation, including high frequency oscillatory ventilation (HFOV) and high frequency jet ventilation (HFJV), which are very commonly used modes for this group of patients. However, there is a lack of this type of capnometer available in the market, which are a must when a patient is intubated to avoid further complications. This is the main reason that gives to this project its value.

The whole process covered:

- Initial design of the capnometer as an independent and open system for possible further development, focusing on the individual components needed for subsequent implementation.
- Implementation of the designed system and verification of the functionality of its individual components.
- Implementation of LabVIEW software and data acquisition system, allowing to obtain and analyse the signal produced by the CO_2 detector and displaying it in real time.
- For the verification of the device functionality, different tests were performed on it to obtain its characteristics. These tests included: analysis of the zero input signal, analysis of the step response of the system, constant flow test with different CO_2 concentrations, normal breathing and high frequency ventilation.
- Combining the measured values obtained from the tests and from the reference capnometer, a calibration curve was created, where a produced voltage by the sensor is correlated to a specific carbon dioxide concentration.
- Verification of the device´s functionality under high frequency ventilation modes.

4 Methods

Based on the all the previously explained theory and knowledge needed for the development of this project, it is possible to move on to the practical part, focused on the design and subsequent implementation of the mainstream capnometer. For a better understanding of the general idea, a simple block diagram shown in Figure 4.1 was elaborated containing the basic components necessary for the proper functioning of the device. These components are basically: the reference capnometer for the testing and calibration, power and gas sources, the infrared source and detector, the endotracheal tube adapter, an amplifier, an A/D converter and a computer with the software for the process and display of the signal.

This chapter contains a detailed description of each of the components, the reasons why they were chosen, the procedures applied and how the problematic of the project was solved.

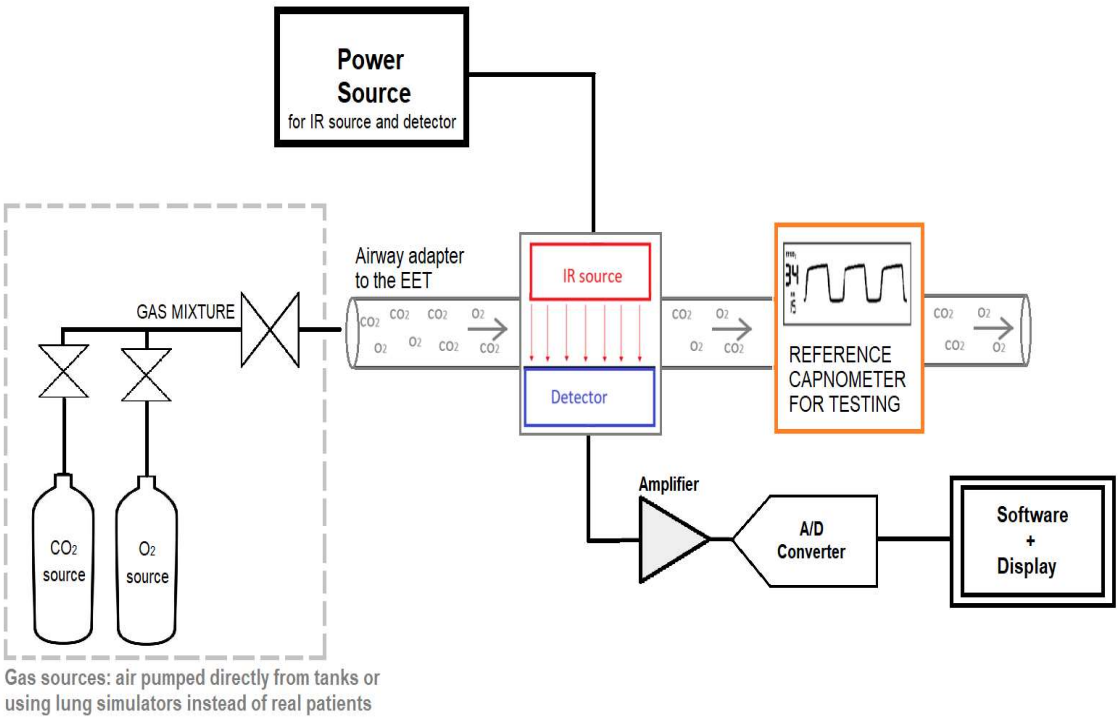

Figure 4.1: General schema of the designed capnometer system

4.1 Infrared source

There is a wide range of different infrared sources available in the market designed specifically for many different types of applications such as thermography, hyperspectral imaging, night vision, tracking, heating, communications, meteorology and spectroscopy.

For the optimal design of the device, it is necessary to establish the most suitable infrared source for output variations as well compensating them for the detector's sensitivity variations due to temperature, external interferences and aging. The main goal of the IR source is to irradiate constantly creating an optimal and highly stable environment for the CO_2 measurements to avoid misleading results.

As explained in Chapter 2.2, there are to main ways to obtain the signal that represent the correlation between the intensity of the IR light and the values of CO_2 concentration. It can be done with or without moving parts (not solid and solid state). The ideal IR source would be one that is capable of being pulsed on and off extremely fast. This capability eliminates the need to interrupt the IR beam with a rotating chopper wheel allowing to implement a solid state sensor, which is preferable due to the lack of moving parts.

There are infrared sources that incorporate an internal component called "beam splitter" that allows a single beam infrared pulse to simultaneously strike reference and measurement detectors, which would be ideal for this case. Another common feature of this types of IR emitters is to use a parabolic reflector to concentrate the IR energy into a focal point increasing its intensity and stability. They usually provide a wide spectrum of emission.

All these requirements for the IR source of the capnometer should be met in order to develop the most accurate design and performance of the device. However, it was very difficult to find such specific source in the market for a low price. For these reasons, the selected option was to recycle an IR source from an old capnometer (CAPNOSTAT 5) available and provided by the faculty´s laboratory.

4.2 Infrared detector

As already mentioned, the best option for CO_2 detection is non-dispersive infrared spectrometry (NDIR). Nowadays, there is a high number and variety of detectors using this principle. Figure 4.2 shows a schematic of the typical NDIR gas sensors.

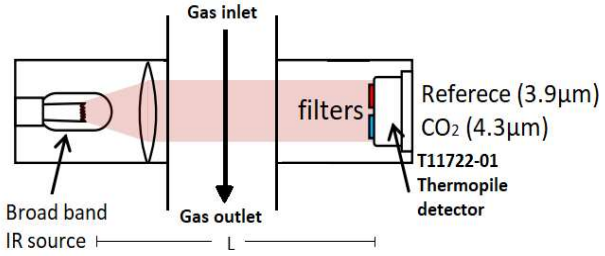

Figure 4.2: NDIR gas sensor schematic. Modified from source [47]

The faculty´s laboratory provided some of the electronic components that could be used for this project. In case of possible detectors, two Indium Arsenide Antimonide photovoltaic detectors (P13243-043MF and P13243-039MF) and one dual-element type thermopile detector T11722-01 from Hamamatsu (manufacturer), designed to detect CO_2 concentration with high accuracy and sensitivity were considered. Main features of each of the options for the detector are described in this chapter.

InAsSb photovoltaic detectors – P13243 Series

The two Indium Arsenide Antimonide photovoltaic detectors suitable for gas measurement, which use a band pass filter with different wavelengths (one use 3,9 µm and the other 4,26 µm). Their rise time is 0,0015 µs and the connection circuit is also the same for both. They also need an amplifier and use a chopper that modulates the optical radiation for fast and very sensitive measurements and of course an infrared source. Main characteristics of the P13243-043MF and P13243-039MF detectors with their recommended circuit proposed by the manufacturer can be observed on Figure 4.3 and Figure 4.4 respectively.

Photosensitive area	0.7×0.7 mm
Number of elements	1
Package category	TO-46, with filter
Package	Metal
Cooling	Non-cooled
Peak sensitivity wavelength (typ.)	4.26 / BPF μm
Photosensitivity (typ.)	0.0031 A/W
Detectivity D* (typ.)	6.9×10^{8} cm · $Hz^{1/2}$/W
Noise equivalent power (typ.)	1.3×10^{-10} W/$Hz^{1/2}$
Rise time (typ.)	0.0015 μs
Terminal capacitance (typ.)	0.7 pF
Measurement condition	Ta=25℃, Detectivity D*: λ=λp, fc=1200 Hz, Δf=1 Hz

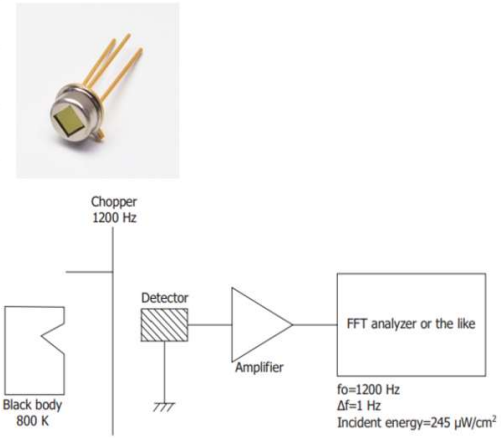

Figure 4.3: P13243-043MF - InAsSb photovoltaic detector main features and measurement circuit diagram proposed by the manufacturer [48]

Photosensitive area	0.7×0.7 mm
Number of elements	1
Package category	TO-46, with filter
Package	Metal
Cooling	Non-cooled
Peak sensitivity wavelength (typ.)	3.9 / BPF μm
Photosensitivity (typ.)	0.003 A/W
Detectivity D* (typ.)	6.5×10^{8} cm · $Hz^{1/2}$/W
Noise equivalent power (typ.)	1.1×10^{-10} W/$Hz^{1/2}$
Rise time (typ.)	0.0015 μs
Terminal capacitance (typ.)	0.7 pF
Measurement condition	Ta=25℃, Detectivity D*: λ=λp, fc=1200 Hz, Δf=1 Hz

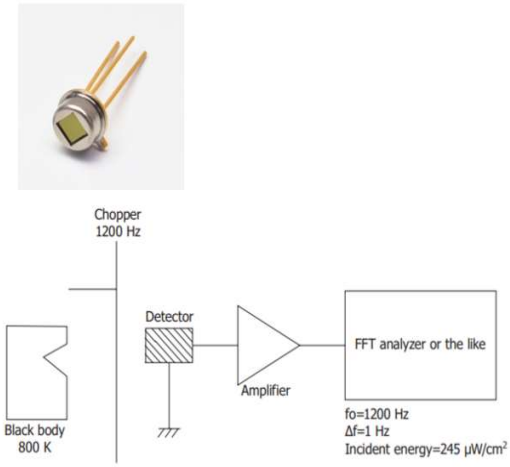

Figure 4.4: P13243-039MF - InAsSb photovoltaic detector main features and measurement circuit diagram proposed by the manufacturer [49]

T11722-01 Thermopile detector

The T11722-01 is a dual-element thermopile detector designed to detect CO_2 concentration with high accuracy. It consists of a high sensitivity dual-element thermopile detector and two band pass filter for sensing two wavelengths simultaneously (one is the reference centred at 3,9 microns and the other for CO_2 reading at 4,3 microns). The reference filter is used to eliminate measurement errors caused by a number of undesirable phenomena such as water vapour caused by exhaled air. It is set to 3,9 microns where no gas components may affect the measured value. In the case of this detector of CO_2 concentration, the recommended circuit connection by the manufacturer use one LTC1050 amplifier because the output signal is very small (in the order of microvolts) and needs to be amplified by using an amplifier with low offset voltage. The main characteristics and the recommended circuit by the manufacturer is shown in Figure 4.5. It has high sensitivity and accuracy and the typical rise time is 20 ms and the maximum is 30 ms. By determining the individual values of resistance and capacitor directly we affect the operating characteristics of the equipment.

Package	Metal
Photosensitive area (per one element)	1.2 x 1.2 mm
Spectral response range	3.9 to 4.3 μm
Photosensitivity (typ.)	50 V/W
Dark resistance (typ.)	125 kΩ
Output noise voltage (typ.)	45 nV/Hz$^{1/2}$
Noise equivalent power (typ.)	0.9 nW/Hz$^{1/2}$
Detectivity (typ.)	1.3 x 10^8 cm · Hz$^{1/2}$/W
Rise time (typ.)	20 ms
Rise time (max.)	30 ms
Temperature coefficient of element resistance (typ.)	±0.1 %/°C

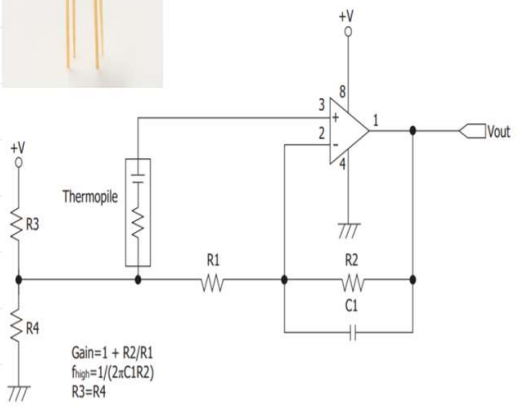

Figure 4.5: T11722-01 Thermopile detector main features and measurement circuit diagram proposed by the manufacturer [50]

It was mentioned before that carbon dioxide absorbs infrared radiation mainly in three narrow bands of wavelengths, which are 2.7, 4.3 and 15 micrometres, so this aspect needs to be taken into account to select the most appropriated components for the most accurate measurement.

Table 4.1: Main features comparison between possible CO_2 detectors

DETECTOR	Centre wavelength	Internal resistance	Rise time	Frequency	Element type	State
T11722-01	3,9 μm 4,3 μm	125 kΩ	20 ms	50 Hz	Dual	Solid
P13243-043MF	4,26 μm	300 kΩ	15 ns	666,66M Hz	Single	Not Solid
P13243-039MF	3,9 μm	300 kΩ	15 ns	666,66 MHz	Single	Not Solid

According to Table 4.1 and regarding to the proximity of the wavelength centres of the detectors and the CO_2, the thermopile would be more convenient because its centres are closer to the CO_2 ones. However, another important aspect to consider is the frequency ranges. The Indium Arsenide Antimonide photovoltaic detectors can perform with higher frequency ranges than the thermopile, but with 50 Hz should be enough for this purpose. Moreover, the thermopile is a dual element type while the other detectors are single type, this means that the thermopile can work with two different wavelengths at the same time, one as a reference and the other one for reading. There are no gas absorption lines at 3,9 – 4,0 microns, enabling the reference signal to be taken at this wavelength, while the other filter coincides with the absorption line of the CO_2 absorption spectrum at 4,3 microns. Additionally, it is a solid sensor (no moving parts needed). For these reasons the T11722-01 Thermopile detector was chosen as the most optimal. Diagrams from manufacturer are presented in Figure 4.6 and Figure 4.7.

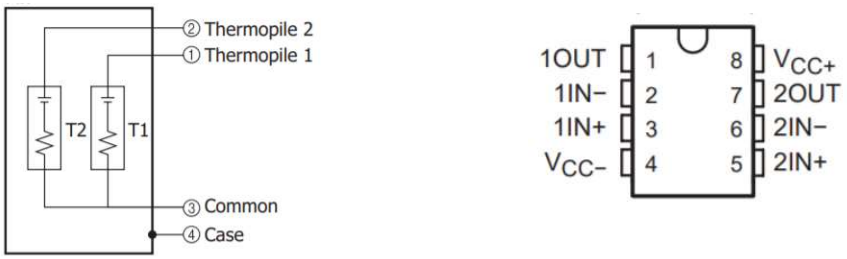

Figure 4.6: Internal disposition of the dual-element thermopiles in the T11722-01 sensor (left) and the top view schematic of the LTC1050 amplifier with the pin distribution for both signals and the power source (right) [50]

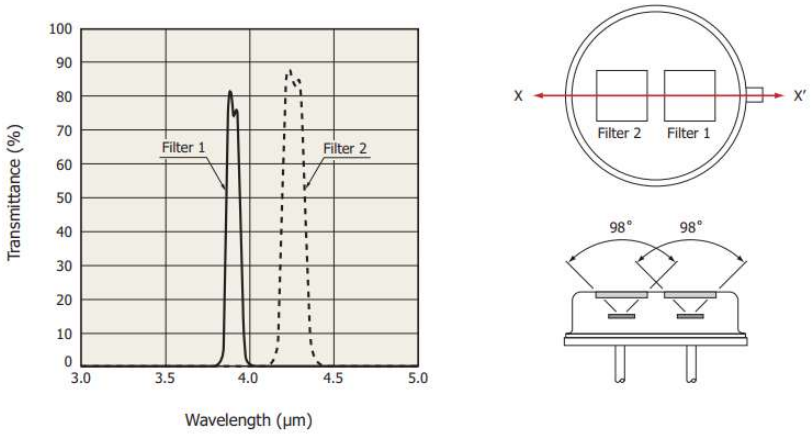

Figure 4.7: Spectral transmittance characteristics, angle and field of view of Hamamatsu T11722-01 detector [50]

Filters are used to suppress unwanted wavelengths that do not carry any useful information. Most often they are part of the detectors themselves, which are made directly from the manufacturers indicating for what wavelengths they are able to filter.

In the case of the Hamamatsu detector, the recommended circuit connection is used with amplifier LTC1050 as shown in Figure 4.8. By specifying the individual values of the resistance and the capacitor directly we influence the operational characteristics of the device.

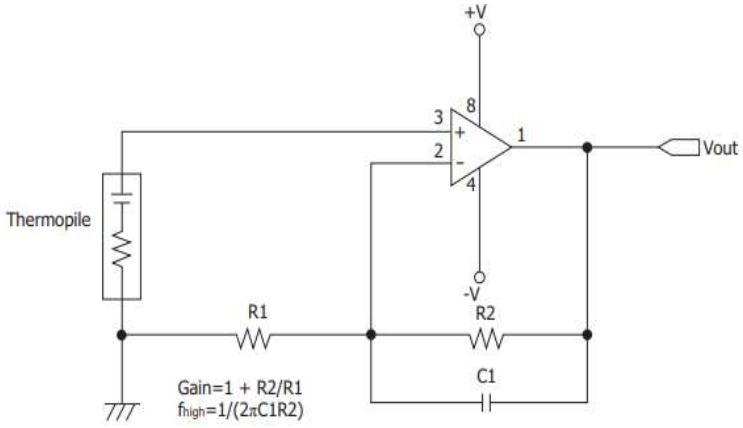

Fig 4.8: Operating circuit of the Hamamatsu T11722-01 detector [50]

The internal resistance of the sensor is 125 kΩ in both channels and the response speed is 20 ms (50 Hz). By changing the external capacitor and resistors (R2 and R1), it is possible vary the amount of gain and the speed of response, which can be a desired phenomenon. It is clear from the diagram that it is a low-pass filter. The capacitor is connected in parallel with the resistor (R2). To calculate the cut-off frequency the next formula is used:

$$f_{cut} = \frac{1}{2\pi RC} = \frac{1}{2\pi \cdot 4.72nF \cdot 1M\Omega} \approx 159Hz \quad (4)$$

The cut-off frequency indicates the value of the frequency at which the gain drops by about 30%. A cut-off frequency of 159 Hz does not cause any loss of information. For successful normal breathing analysis is sufficient from 5 to 10 samples per second. The output voltage value from the sensor is in the order of μV, so it is amplified using the LTC1050 amplifier. The output amplified signal is then connected to the analogue-to-digital converter (DAQ system explained in chapter 4.5). Figure 4.9 shows a diagram of the implemented circuit for the CO_2 detector.

Gain can be calculated using the next formula:

$$GAIN = 1 + \frac{R2}{R1} = 1 + \frac{1M\Omega}{1k\Omega} = 1 + \frac{1 \cdot 10^6}{1 \cdot 10^3} = 1001 \quad (5)$$

With the calculated gain, the output voltage produced by the sensor is increased from the order of μV to the order of mV, facilitating in this way to be detected, recorded and further process of the signal.

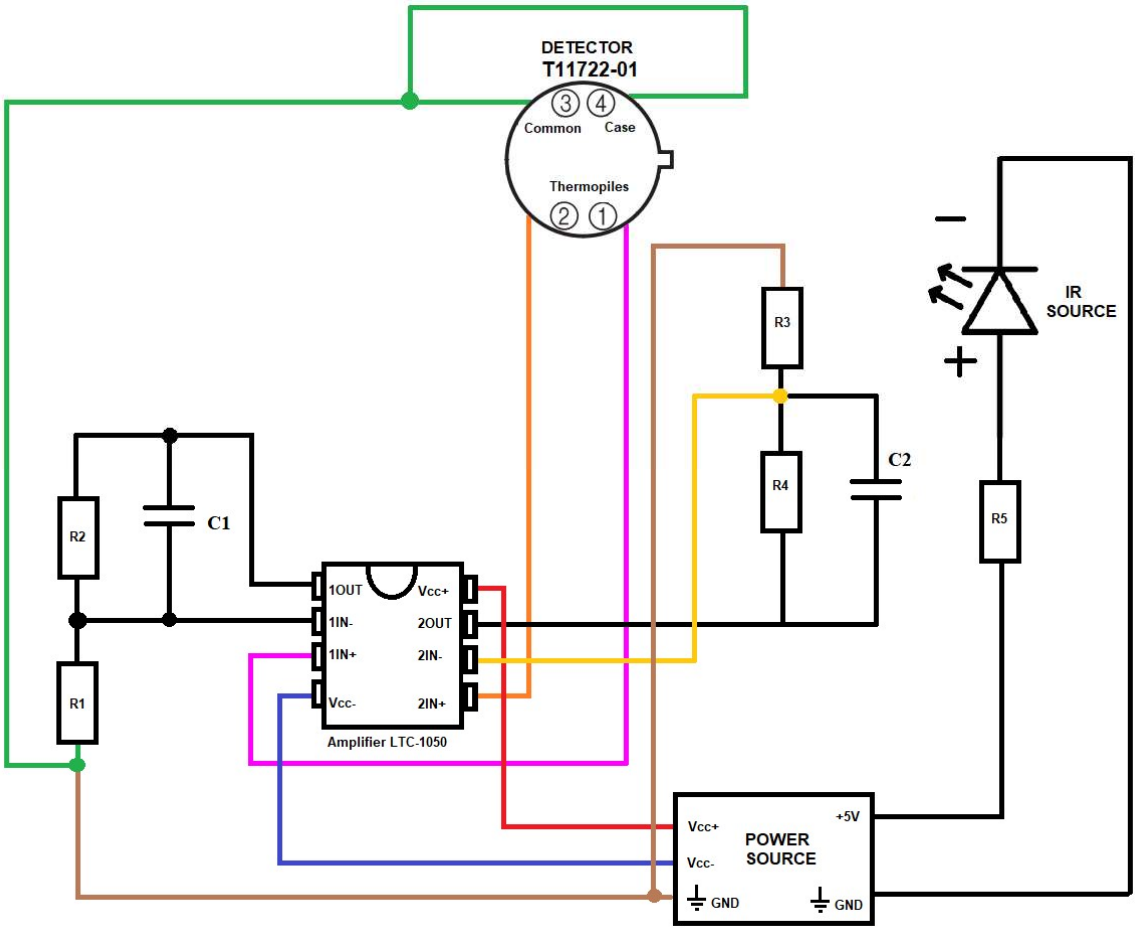

Figure 4.9: Diagram of the implemented circuit for the CO_2 detector

4.3 Airway adapter

The selected mainstream endotracheal tube adapter is typically used and was provided by the faculty and it has two different configurations. For the neonatal breathing circuit there is a smaller diameter opening inside, while the bigger diameter is for adults, as observed on Figure 4.10:

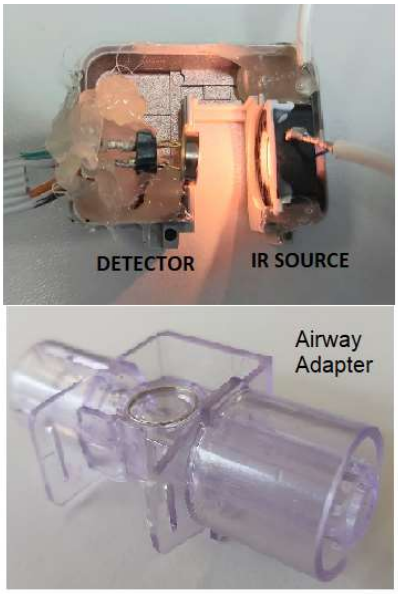

Figure 4.10: Airway adapter configuration

Both the source and the IR radiation sensor are built into the cuvette itself, to eliminate undesirable environmental influences. The cuvette has to be made of a suitable material, which is permeable to optical radiation. Most often they are made of glass, metal or in this case, plastic. It was the selected option because it presents good temperature resistance and the ability to implement the infrared source and detector on both sides of the wall of the tube (windows) also due to their temperature and chemical stability in contact with gas. The advantage is also easy availability and low acquisition costs. Detecting windows are indispensable for CO_2 monitoring because it allows the light beam to pass through the airway adapter to the measuring chamber. Depending on the gas concentration, there are different lengths of the cuvettes, but due to the high density of CO_2 molecules, which are exhaled by the patient, cuvettes up to 5 cm long are used.

The optical path is the trajectory that a light ray follows as it propagates through an optical medium. In this case the optical path is between the radiation source and the detector. Radiated infrared rays pass through a number of individual components of the device, each of which is made up of different materials and therefore have different optical properties, which in total are reflected in the resulting luminous flux. But ideally, individual rays would only change its wavelength depending on the concentration of CO_2 molecules and consequently allowing their detection and quantification.

4.4 Data acquisition

Data acquisition is defined as the process of sampling signals that measure real world physical conditions and converting the resulting samples into digital numeric values that can be operated by a computer. Data acquisition systems (DAQ) usually convert analogue signals into digital values for further processing by using software programs such as Assembly, BASIC, C, C++, C#, Fortran, Java, LabVIEW, Lisp, Pascal, etc.

It is possible measure a huge number of different parameters using a DAQ system. The most common ones are voltage, current, temperature, strain, pressure, vibration, distance, angles, revolutions per minute, weight, digital signals and frequency or time intervals. Figure 4.12 shows a basic block diagram of the digital data acquisition system.

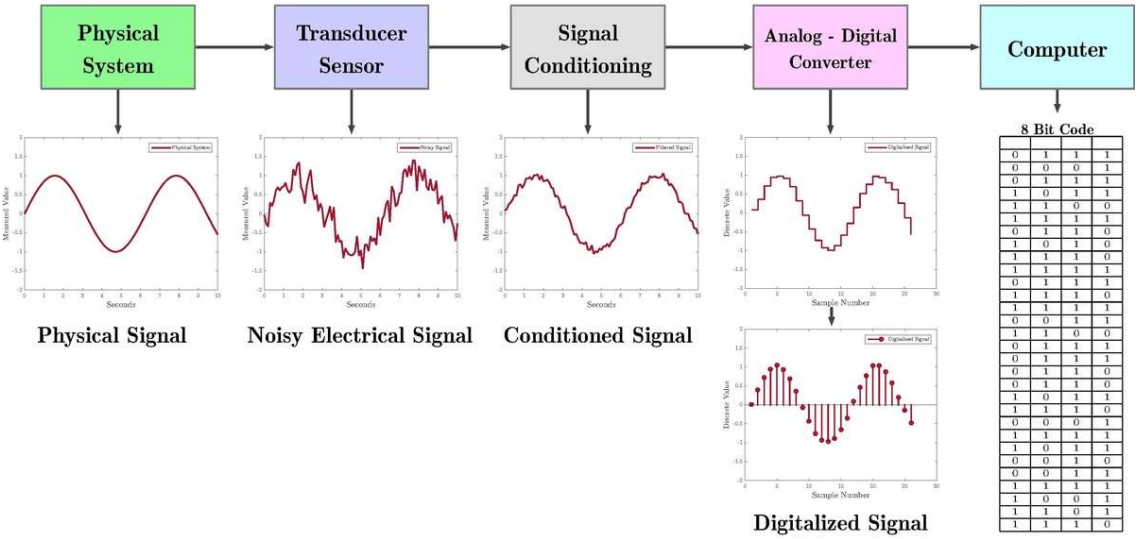

Figure 4.12: Digital Data Acquisition System Block Diagram [51]

NI-DAQmx (Figure 4.13) is an instrument that controls every aspect of the DAQ system, including signal conditioning, from configuration to programming in LabVIEW to low-level OS and device control. It can build many different applications with measurement-specific functions, data types, and analysis integrations and reliably make faster measurements. NI-DAQmx supports NI LabVIEW, SignalExpress, C/C++, Visual Basic and C#. Along with LabVIEW, NI-DAQmx is one of the main reasons National Instruments is a leader in virtual instrumentation and PC-based data acquisition.

Figure 4.13: Multi-channel data acquisition module NI-DAQmx

4.5 Software and Display

The software used for this project was Laboratory Virtual Instrument Engineering Workbench known as LabVIEW, which is a graphical programming environment engineers use to develop automated research, validation, and production test systems. The software license was provided by the faculty and the developer of the software is National Instruments. LabVIEW is commonly used for data acquisition, instrument control, and industrial automation on a variety of operating systems (Microsoft Windows, Unix, Linux, and macOS). It was first launched in 1986 as a tool for scientists and engineers to facilitate automated measurements. It uses a graphic interface that enables different elements to be joined together to provide the required flow providing a powerful platform for a wide variety of different applications. It started as an environment for managing test programming, but since its beginning, the applications for which it can be used have considerably expanded from being a graphical test management language to become a graphical system design environment. Some of the advantages of this software are: its flexible and simple interface, it is a universal platform, it has many uses with different external hardware (data acquisition, test equipment…) and it is widely implemented.

LabVIEW incorporates the formation of user interfaces (called front panels) into the development cycle. LabVIEW subroutines are called virtual instruments (VIs). Each VI is composed of three elements: a block diagram, a front panel (built using controls and indicators), and a connector pane (to represent the VI in the block diagrams). Controls are inputs, allowing the user to supply information to the VI. While indicators are outputs, displaying the results based on the given inputs. The back panel, which is a block diagram, contains the graphical source code. Every object placed on the front panel will appear on the back panel as terminals, as it is shown in Figure 4.14, with the back panel or block diagram on the left and the front panel on the right. The back panel also contains structures and functions which perform operations on controls and supply data to indicators. Each VI can be easily tested before being embedded as a subroutine into a larger program.

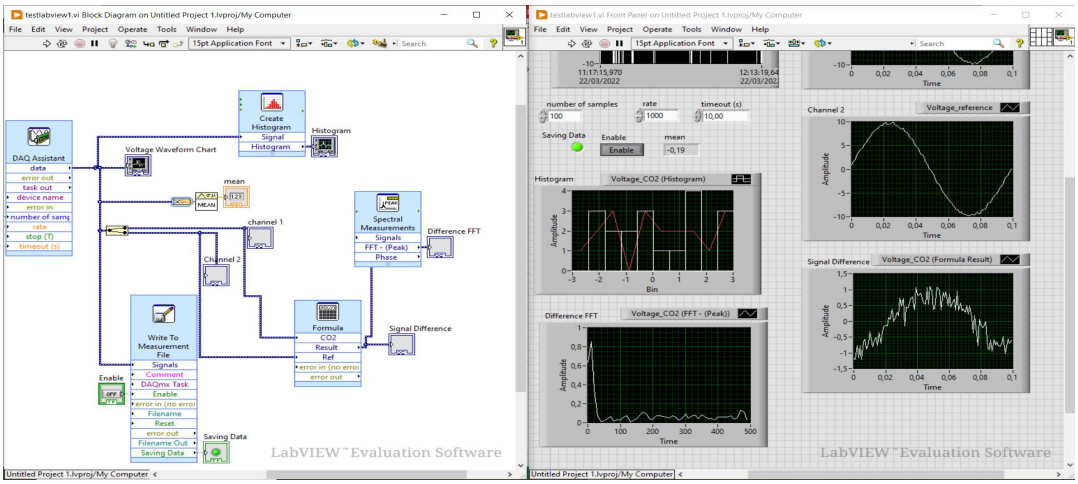

Figure 4.14: LabVIEW front panel (right) and block diagram (left)

The back panel incorporates one relevant function called “DAQ assistant” that easily allows the user to get the output signals from the connected DAQ module by setting the signal with its pin number, setting the maximum and minimum voltage, the acquisition mode (one sample, N samples or continuous samples), the terminal configuration (differential or reference single ended) and the sampling frequency (at least two times the value of the signal frequency), as observed in Figure 4.15:

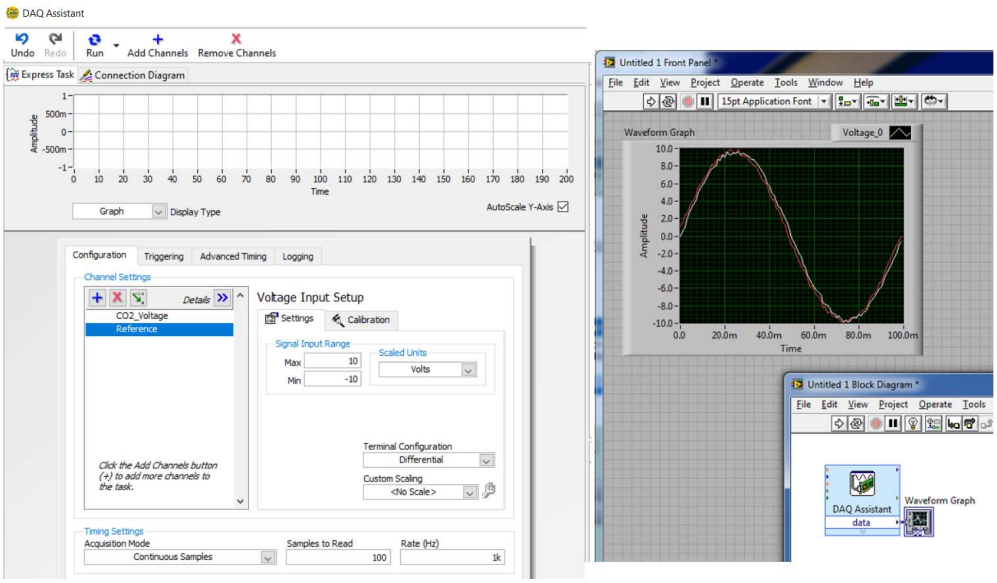

Figure 4.15: DAQ assistant configuration

Once the DAQ assistant is set, the raw output signal can be easily visualized by a graph indicator that displays the signal in real time. However, the raw signal needs to be filtered and processed first in order to obtain the correlated CO_2 concentration signal which is the main purpose of this project. In LabVIEW filtering can be achieved by another function that takes the raw signal as input and provides the filtered one as output. Filters can be easily configured selecting the type of filter, the cut-off frequency and other specifications as shown in Figure 4.16. Once the filter is established, the filtered signal can be display simply by a graph indicator.

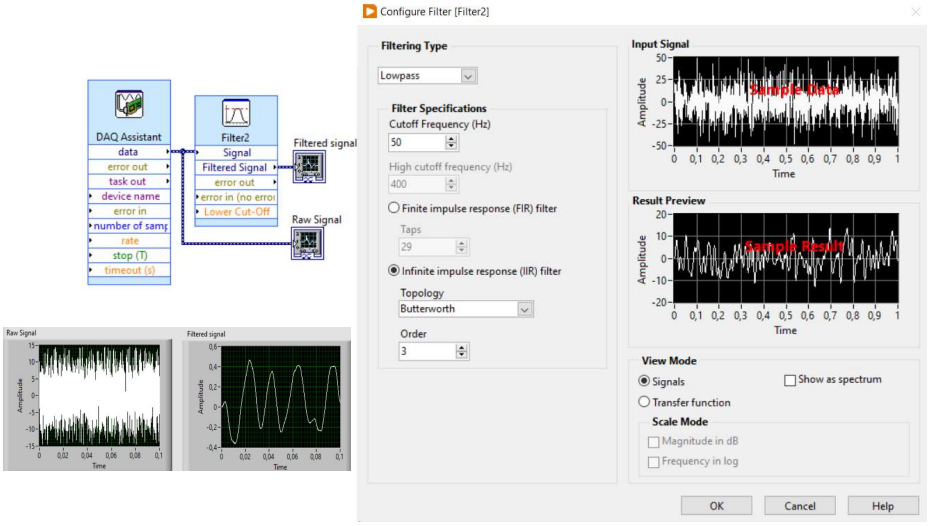

Figure 4.16: Configuration and display of filter function in LabVIEW

Another interesting function called spectral measurements, performs FFT-based spectral measurements, such as the averaged magnitude spectrum, power spectrum, and phase spectrum on the signal as observed in Figure 4.17.

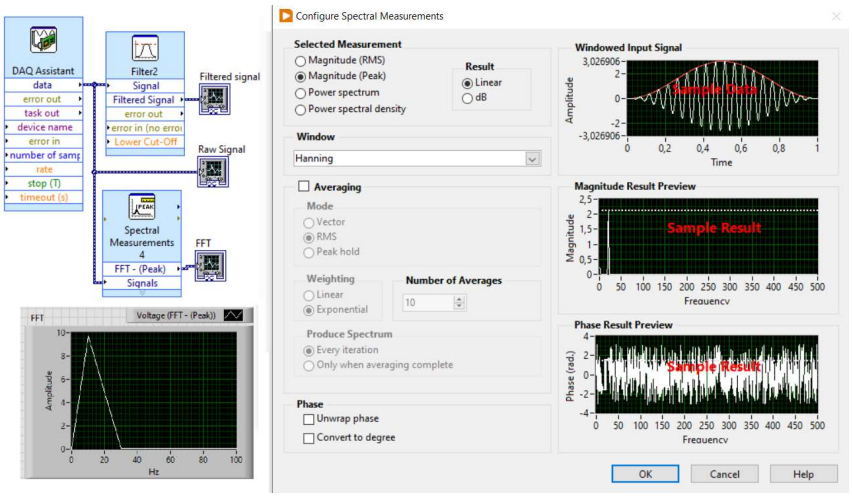

Figure 4.17: Spectral measurements configuration LabVIEW

Different functions and methods were implemented trying to extract the desired signal from the raw signal first such as Hilbert Transform function, envelope detection and peak detection function. However, the results obtained with them were discarded until it was found one approach that allowed to optimally visualize the produced signal as it can be observed in Figure 4.18 by using a mean signal generator.

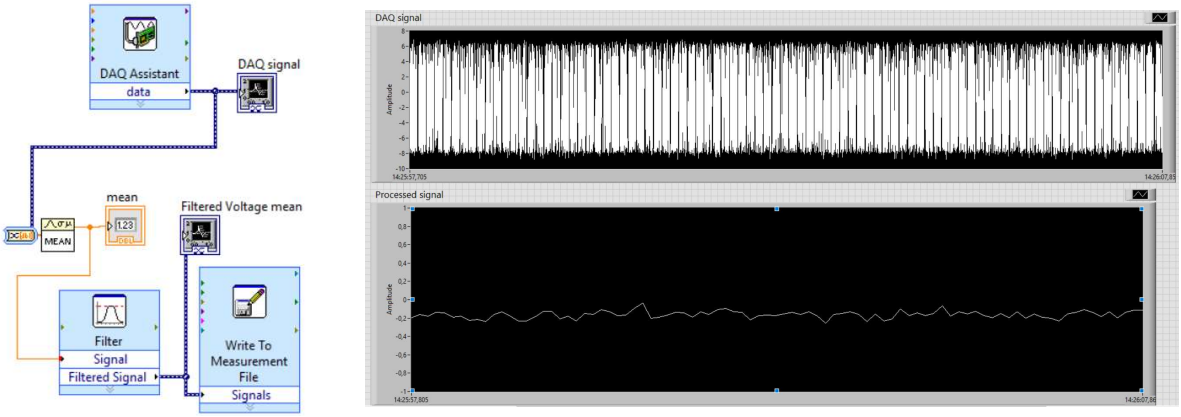

Figure 4.18: Simple method to visualize the raw signal (upper display) and the processed signal (lower display) in LabVIEW

After the successful implementation of the software, the following chapter deals with the testing and verification of the device´s functionality. First of all, basic measurements procedure for obtaining the measured data is described, which are then analysed. The CO_2 detector must be properly calibrated, thus, a calibration curve must be generated in order to optimize the measured results.

5 Testing

This chapter deals with the experiments that were conducted on the implemented system after incorporating some initial improvements based on the preliminary testing. These initial testing and improvements included:

- Supplying power to the CO_2 sensor and the infrared light source separately.

- Verify the correct functioning of the infrared source, the detector, the DAQ system and the software individually. This task was performed using a voltmeter, an oscilloscope and the computer.

- After successful testing of the basic properties of the individual parts, the detector and infrared source were mounted in a small case using a recycled capnometer case that is used because of its easy handling and appropriate protection. The device is created for the purpose of further development, therefore it is possible to access to the inner part of the case.

- Analyse the static and dynamic output signals of the detector and generate signals simply by blowing to the sensor, changing the CO_2 concentration and verifying the acquisition of the produced signal. For this purpose, an auxiliary software called DAQexpress was used first to visualize and manipulate the generated signals easily.

- The airway adapter could then be inserted into the holder too. It was observed a decrease in the amplitude and sensitivity of the signals when the adapter was placed due to its own absorption that has to be considered. For this reason, it was necessary to drill the window next to the detector with a small hole so the absorption of the cuvette can be dismissed because the sample is now in direct contact with the detector. It is very important to ensure the adequate position of the airway window and the sensor inserted in the hole to avoid misleading measurements.

- Verify the correct stabilization and visualization of the output signal using both the active IR source and the airway adapted correctly placed. With these initial settings and improvements implemented and verified, it is possible to move on to the next tests. In Figure 5.1 there is a picture with the whole laboratory setup that was used for this purpose.

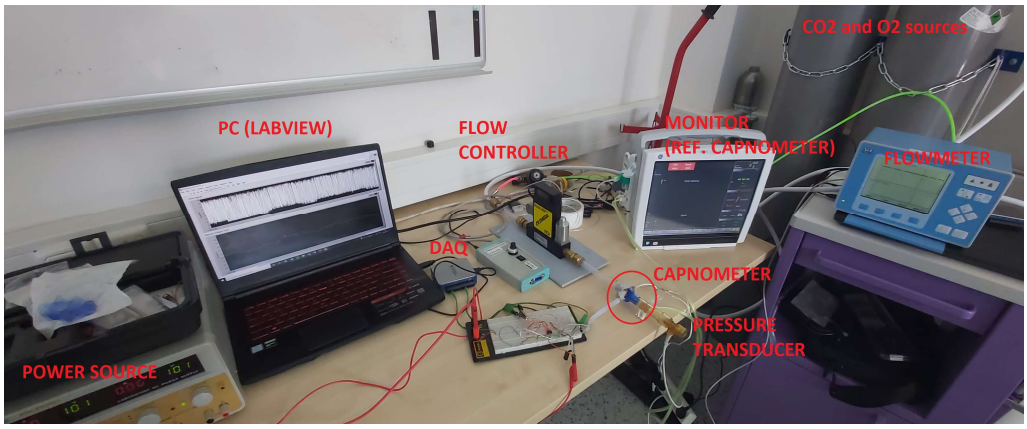

Figure 5.1: Laboratory setup used for static testing of the capnometer

5.1 DAQ Express initial measurements

- Maximum sampling frequency of the DAQ system = 5 kHz
- Cut-off frequency set to 50 Hz
- Voltage range ± 10 V

Zero input reference signal

It can be observed in Figure 5.2 that the reference signal with zero input is approximately constant around 8,85 V. This signal produced by the reference channel is constant and as mention in Chapter 4.3 its filter is centred at 3,9 µm where there is no gas absorption happening and is used to eliminate measurement errors caused by a number of undesirable phenomena such as water vapour.

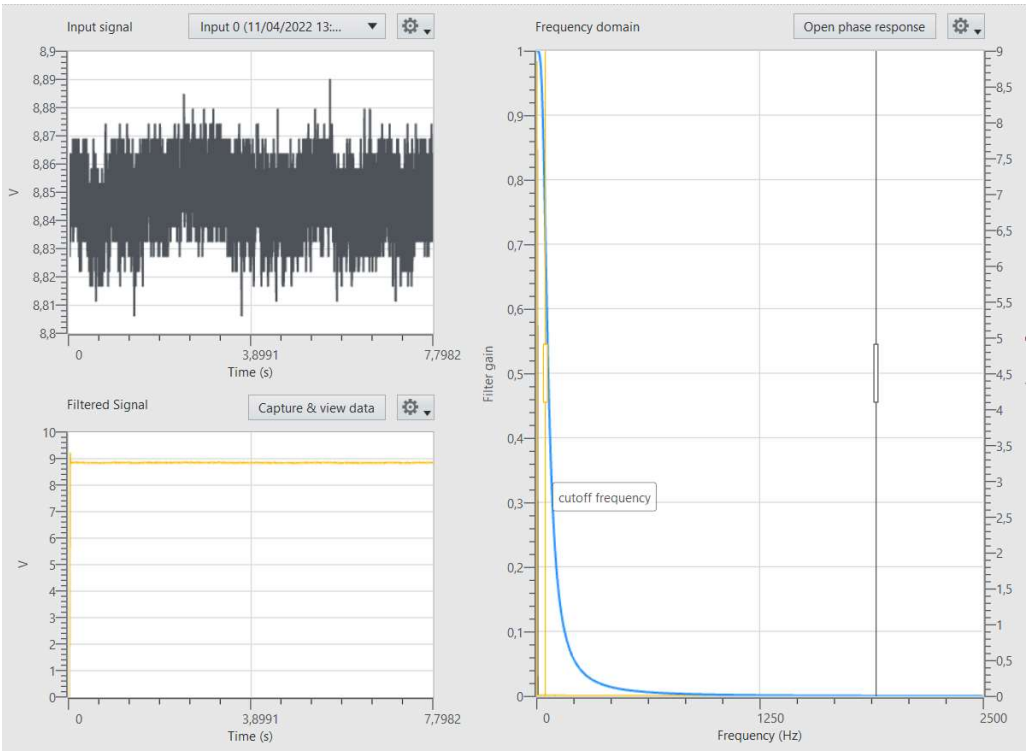

Figure 5.2: Raw and filtered signal from reference channel with zero input

Zero input CO_2 signal

The CO_2 signal with zero input shown in Figure 5.3, is stabilized at -8,86 V and presents bigger fluctuations, due to the fact that although there is no gas flowing, there is some CO_2 concentration present in the air inside the cuvette.

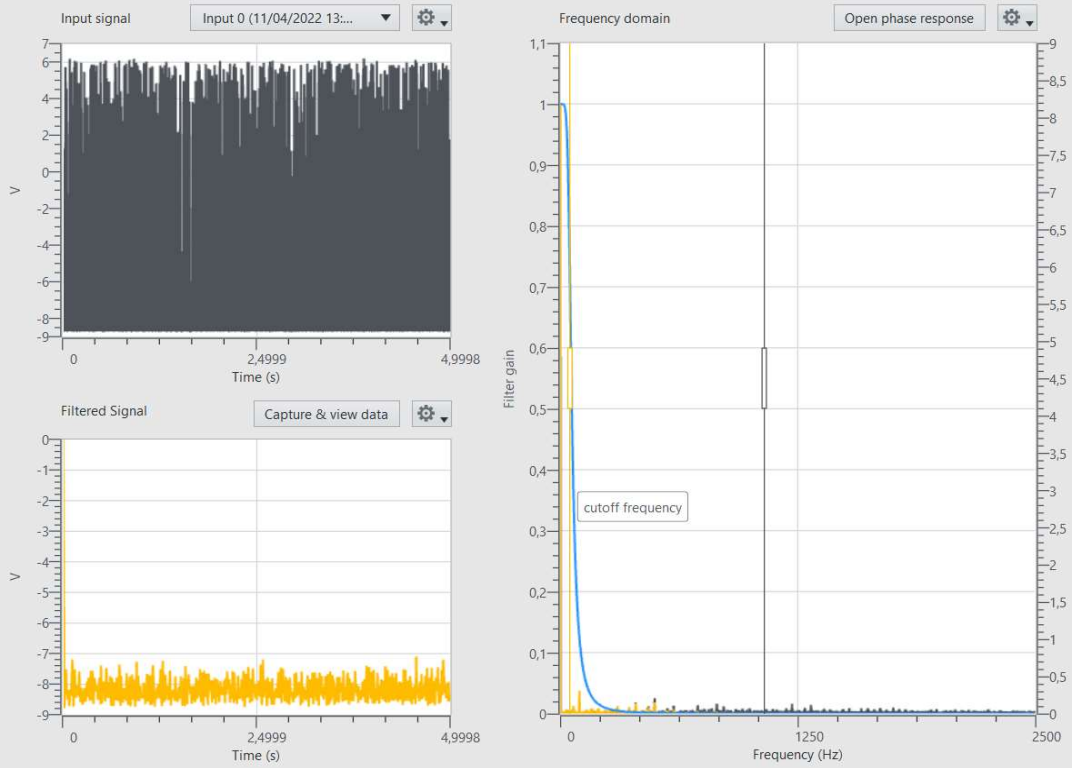

Figure 5.3: Raw and filtered signal from CO_2 channel with zero input

Random CO_2 generated signal:

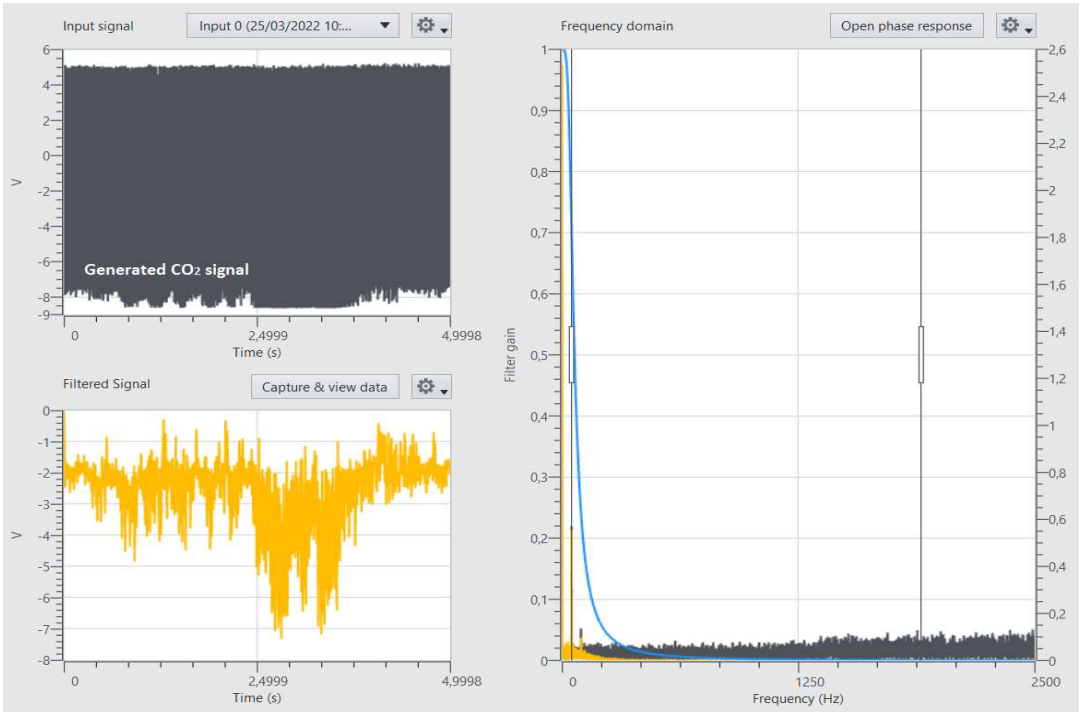

Figure 5.4: Raw, filtered and frequency domain of random CO_2 generated signal

It can be observed from the generated raw signal visualized with DAQexpress in Figure 5.4 and Figure 5.5 that the signal of interest (the voltage changes produced by the difference in CO_2 concentration) corresponds to the envelope of the signal. Thus, the signal needs to be processed using LabVIEW in order to extract the data and produce another signal that contains only the desired information.

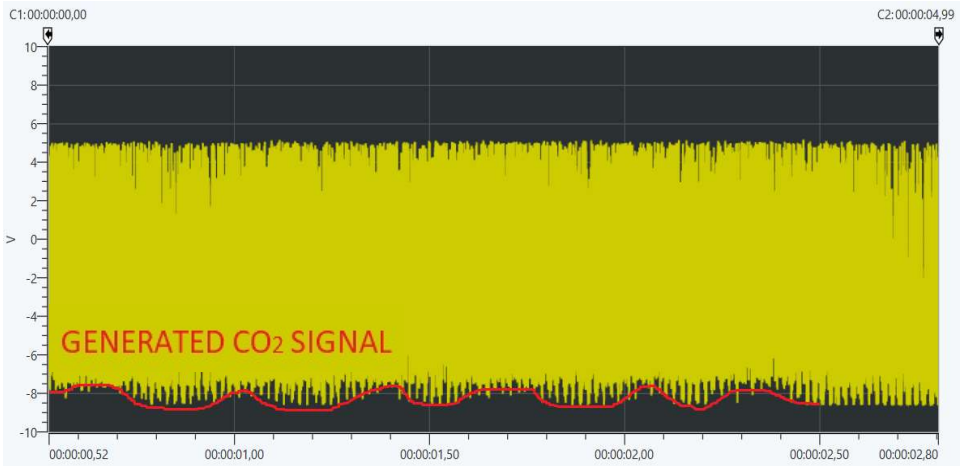

Figure 5.5: Raw signal produced by quickly blowing to the sensor

Once the basic functionality and initial behaviour of the system have been checked with the auxiliary software, it is possible to move forward and perform the next measurements using the implemented program in LabVIEW for further processing and display of the final signal. All measurements were performed under the same conditions. Otherwise, it may occur inaccuracies in the measurements due to different temperature, humidity, pressure or other external factors.

5.2 Static tests

5.2.1 Zero input signal (no airflow)

The first performed experiment was simply to analyse the static output signal of the device when there was no gas flowing inside the airway adapter. It can be expected that very small and practically constant signal can be produced by the sensor due to the small amount of carbon dioxide present in the air (~0.04%). Figure 5.6 shows the LabVIEW front panel with the display of the raw signal coming from the DAQ system and the processed signal.

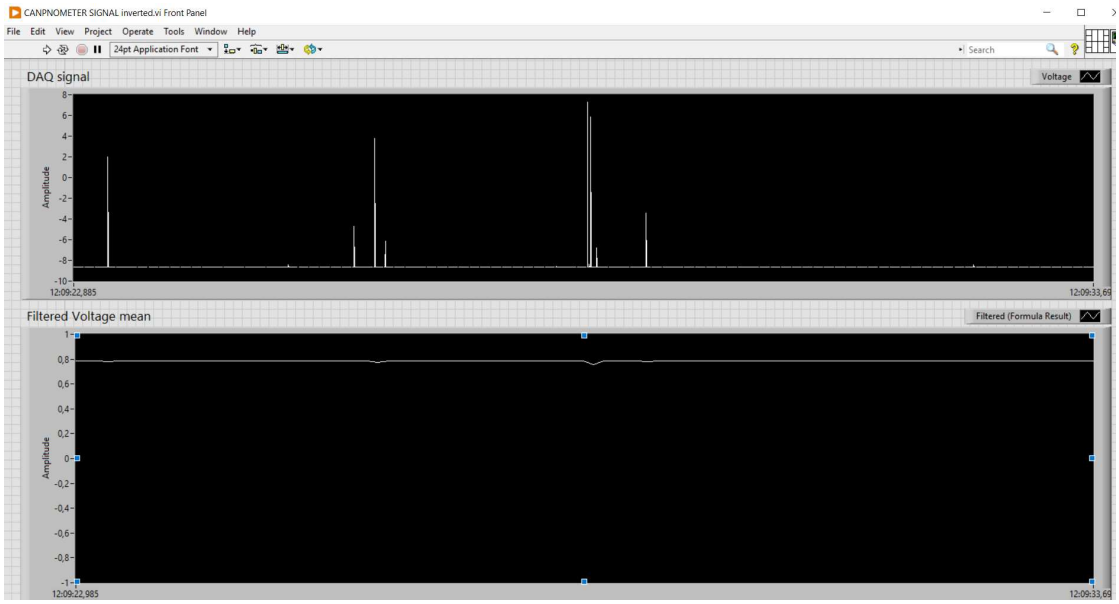

Figure 5.6: LabVIEW front panel, display of the zero input signal (raw signal in the upper display and processed signal in the lower display). Sampling frequency raw signal=100 Hz Sampling frequency processed signal=10Hz

5.2.2 Step response

The step response of a device involves the time evolution of the output when the input is a step function. In other words, the step response is the time behaviour of the output when the input change from zero to one in a very short time (as observed in Figure 5.8). The main goal of this test is to evaluate the step response of the system and obtain the response time of the final signal plus the voltage difference produced.

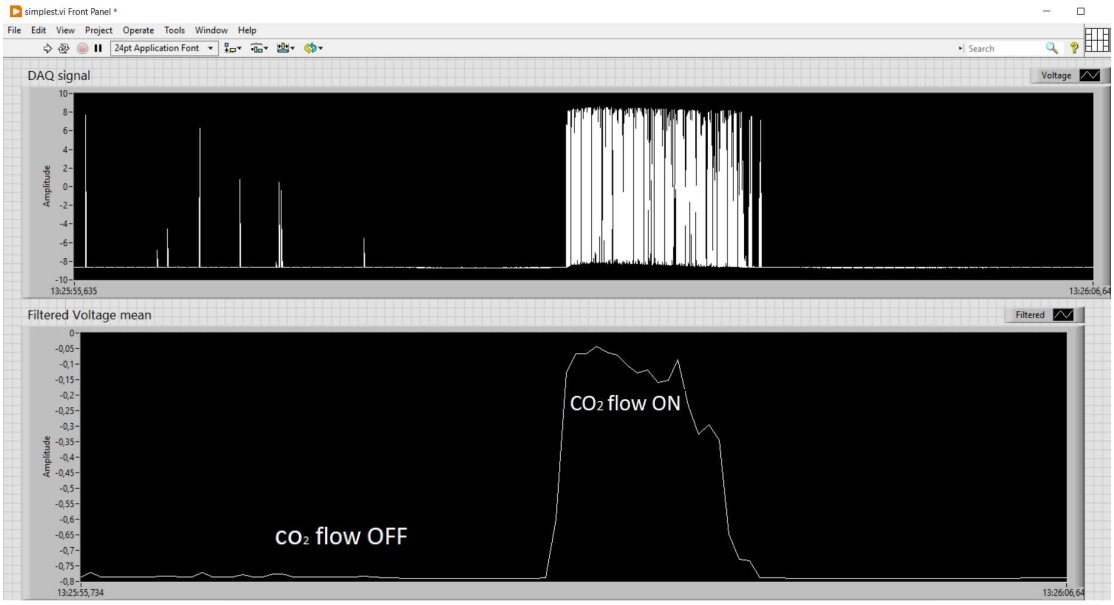

Figure 5.8: Display of step response signal of the device

5.2.3 Constant CO_2 with different flow rates

In order to analyse the signal that the detector produces when the concentration of CO_2 is constant (CO_2 % measured by reference capnometer), an external carbon dioxide gas source was used together with a flow meter to provide a constant flow rate during this experiment. Each test was performed using the same CO_2 concentration (5%) but with different flow rate. The goal of this test was to observe the response of the system under the different flow rates but with the same CO_2 concentration in order to obtain information about how changes in the flow rate affects the CO_2 measurements. The tests were performed using a range of flow rates from 15 Lpm (litres per minute) to 1 Lpm as it can be observed in Figure 5.9.

15 Lpm

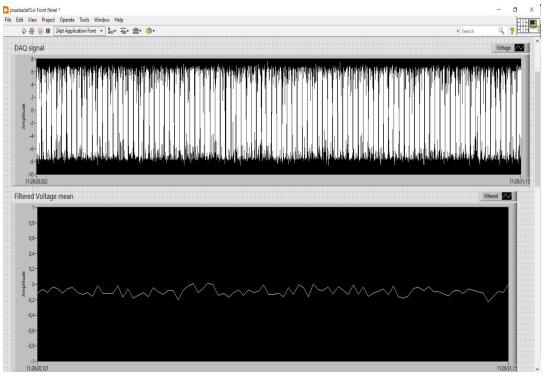

10 Lpm

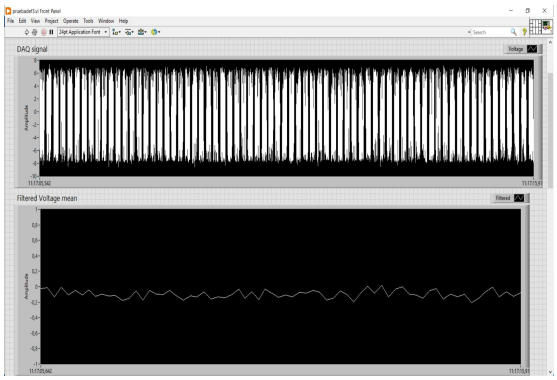

5 Lpm

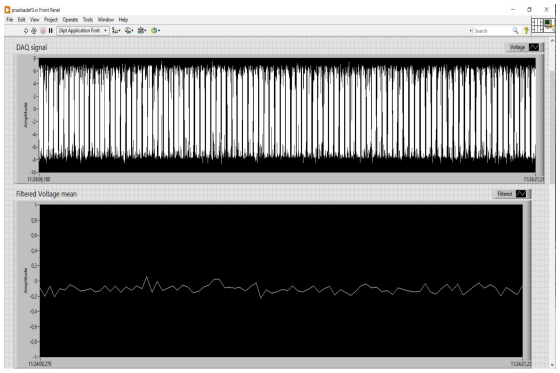

2 Lpm

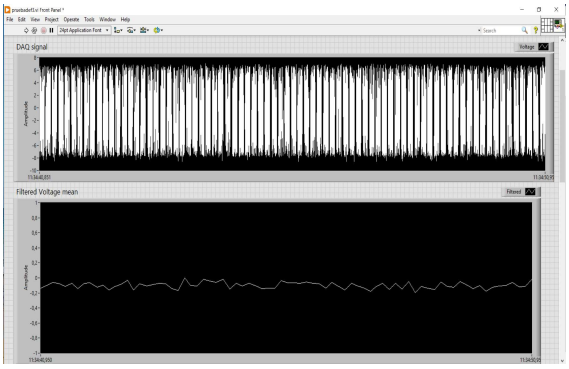

1 Lpm

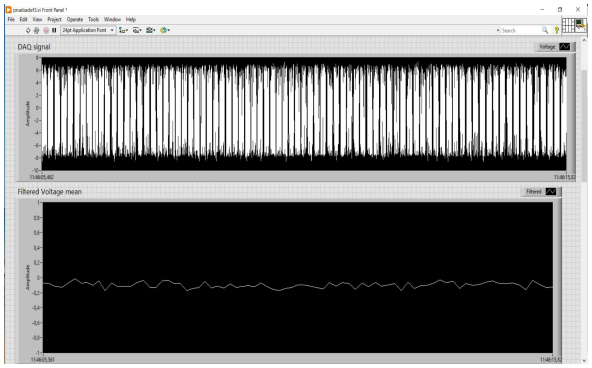

Figure 5.9: Displayed signals with constant CO_2 concentration using different flow rates

5.2.4 Normal breathing

Once the static signals produced with zero and constant CO_2 concentration were recorded by the previous tests, next experiment consisted simply into breath normally through the airway adapter and record the produced signal, observed in Figure 5.10, where the exact values of the $EtCO_2$ were confirmed and recorded by the monitor or reference capnometer in order to compare the results after the analysis.

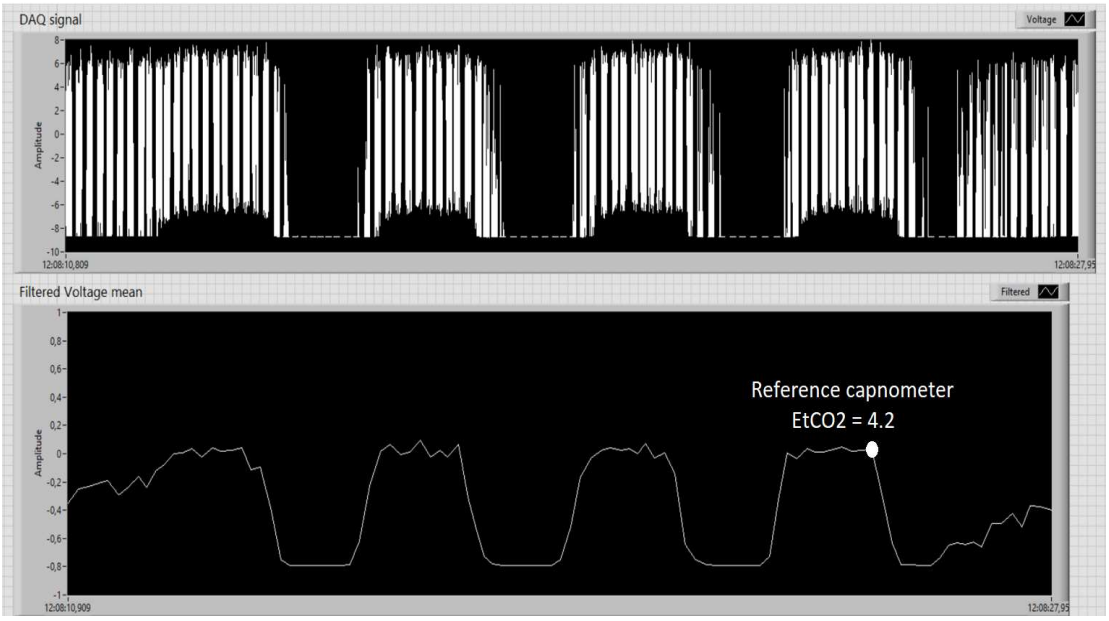

Figure 5.10: Signals produced by normal breathing and $EtCO_2$ read from monitor

Once both capnometers were connected together, the signal produced by conventional breaths were recorded simultaneously, as it can be observed in Figure 5.11, in order to establish further comparison and calibration.

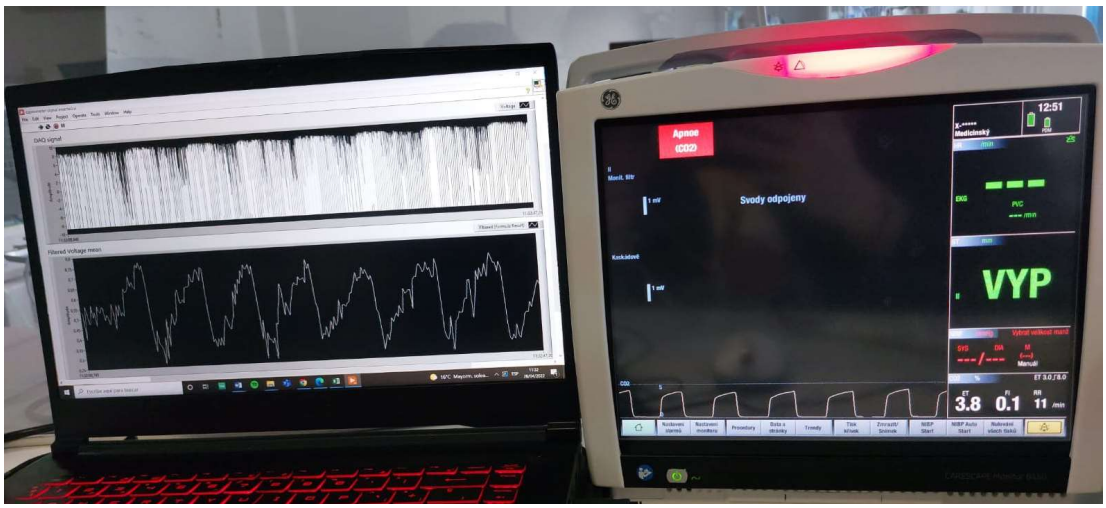

Figure 5.11: Picture of both capnometers working simultaneously

5.3 High Frequency Ventilator testing

Once the static behaviour of the capnometer and its ability to display optimally signals under conventional ventilation have been check by the previous measurements, it is possible to move on to the final type of experiment performed for this thesis, which is to observe the behaviour and functionality of the device under higher respiratory frequencies related to HFV. For this purpose, a high frequency oscillatory ventilator was used (3100A HFOV system from Sensormedic) observed in Figure 5.12 with the rest of the setup. This ventilator easily allows the user to set the desired frequency to be used. As mentioned in Chapter 2.6, HFOV uses from 3 to 15 Hz while HFJV from 4 to 7 Hz.

Figure 5.12: Laboratory setup for high frequency ventilation testing

The first test performed on the device for HFV was with the oscillator set at 5 Hz, the initial display of the oscillations can be observed in Figure 5.13.

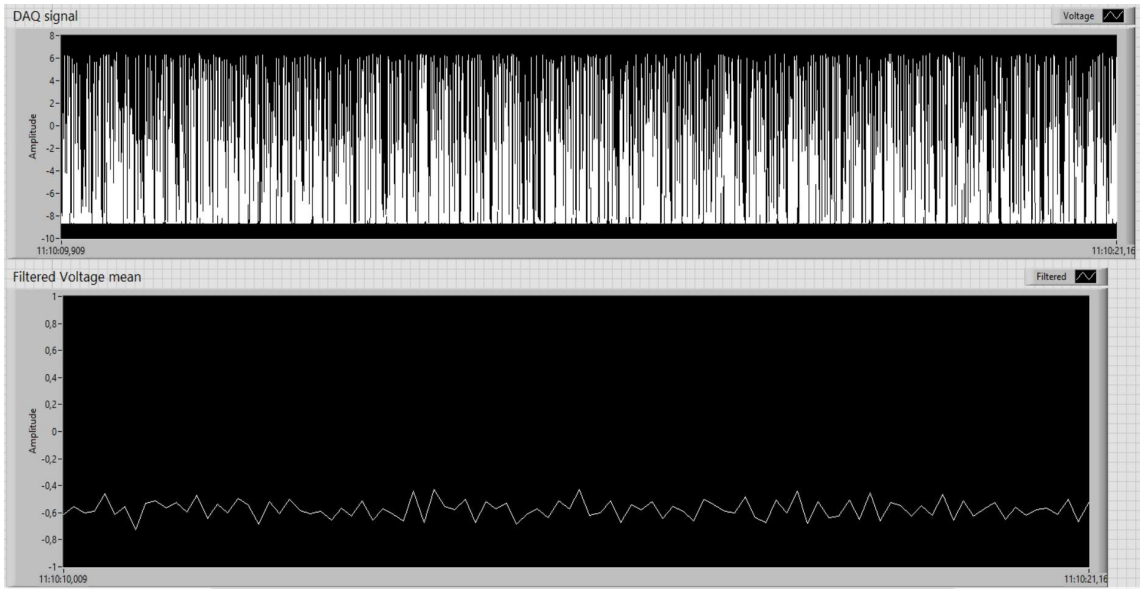

Figure 5.13: Display of the signal using an oscillatory frequency of 5 Hz

Although some small oscillations could be seen initially, for an optimal visualization of the signal it was necessary to escalate it, as observed in Figure 5.14.

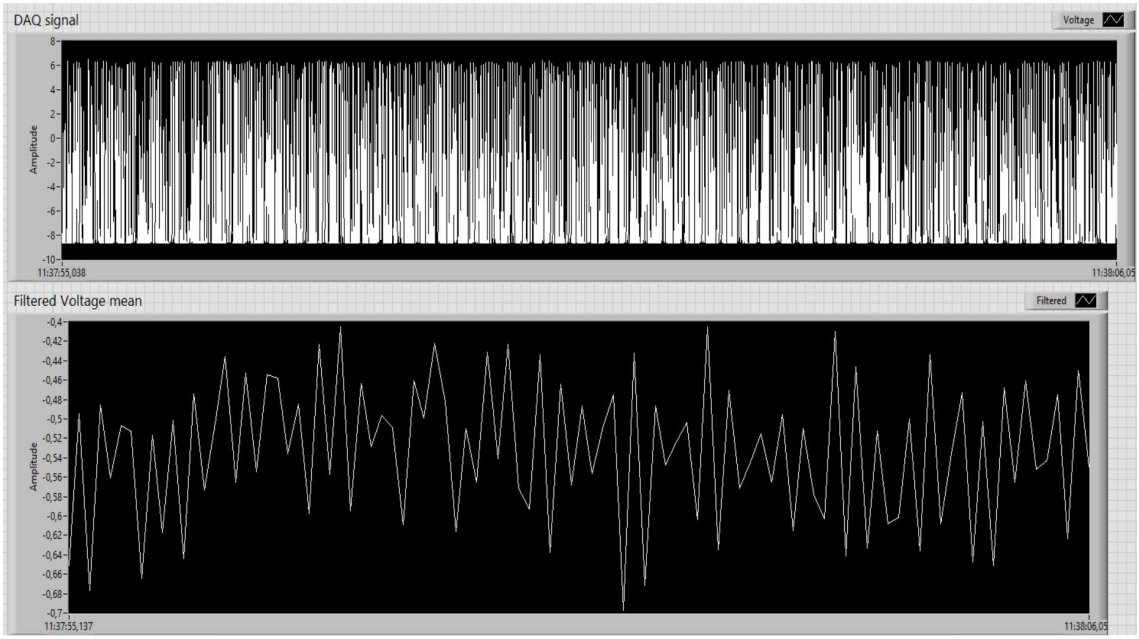

Figure 5.14: Display of escalated signal using an oscillatory frequency of 5 Hz

The following experiments consisted of recording the signal repeatedly when gradually increasing the oscillatory frequency until reaching the maximum of 15 Hz.

The display of the resulting signals for these experiments are shown respectively in the next figures (from Figure 5.15 to 5.19).

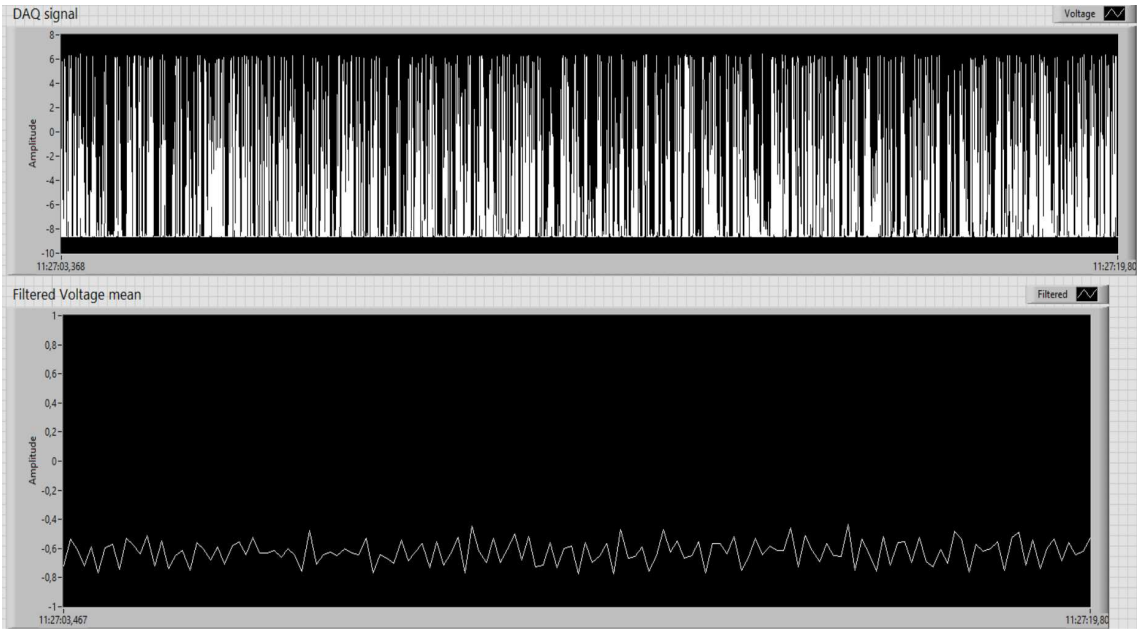

Figure 5.15: Display of the signal using an oscillatory frequency of 5,5 Hz

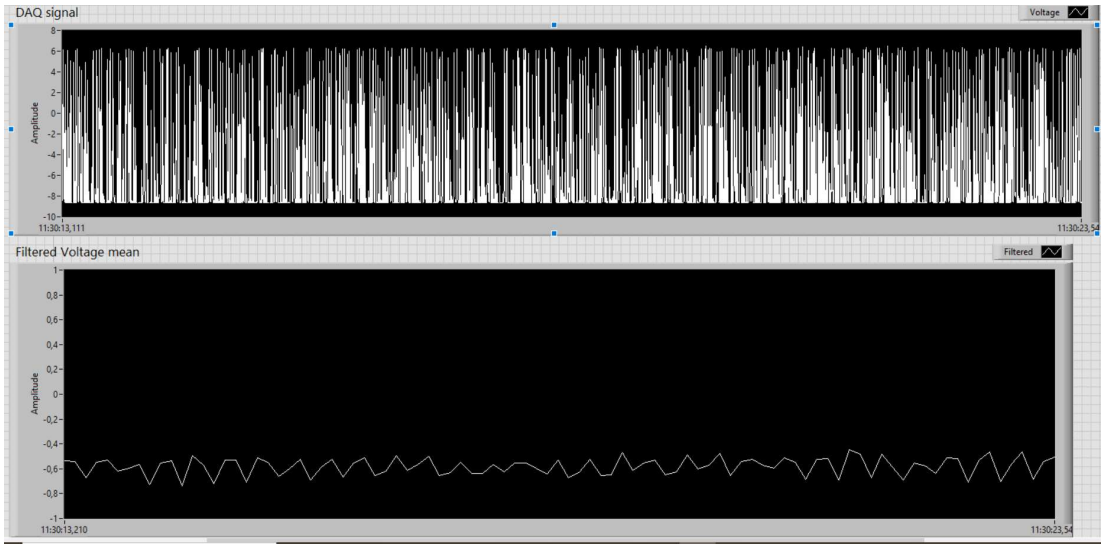

Figure 5.16: Display of the signal using an oscillatory frequency of 6 Hz

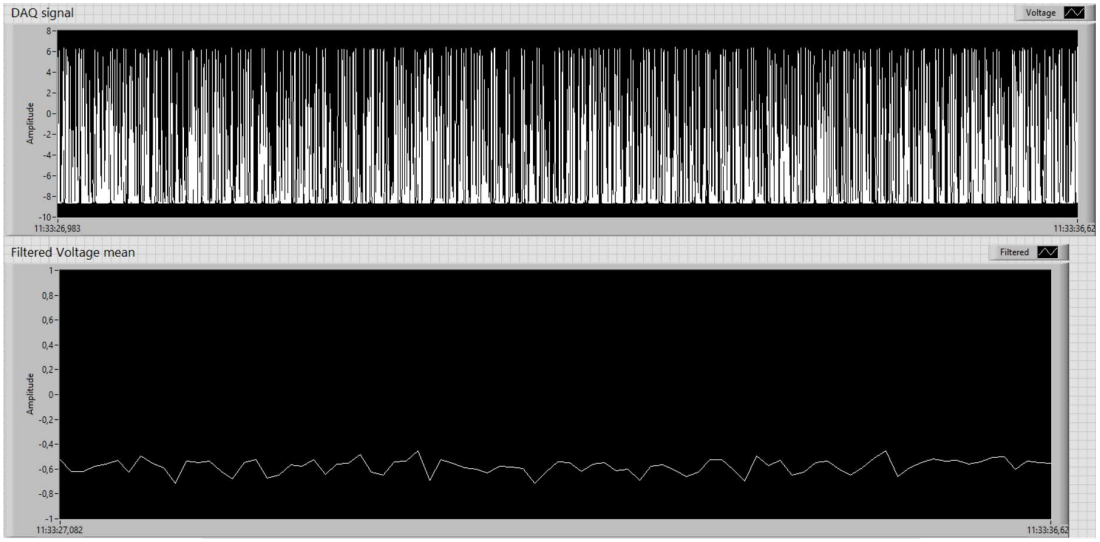

Figure 5.17: Display of the signal using an oscillatory frequency of 7 Hz

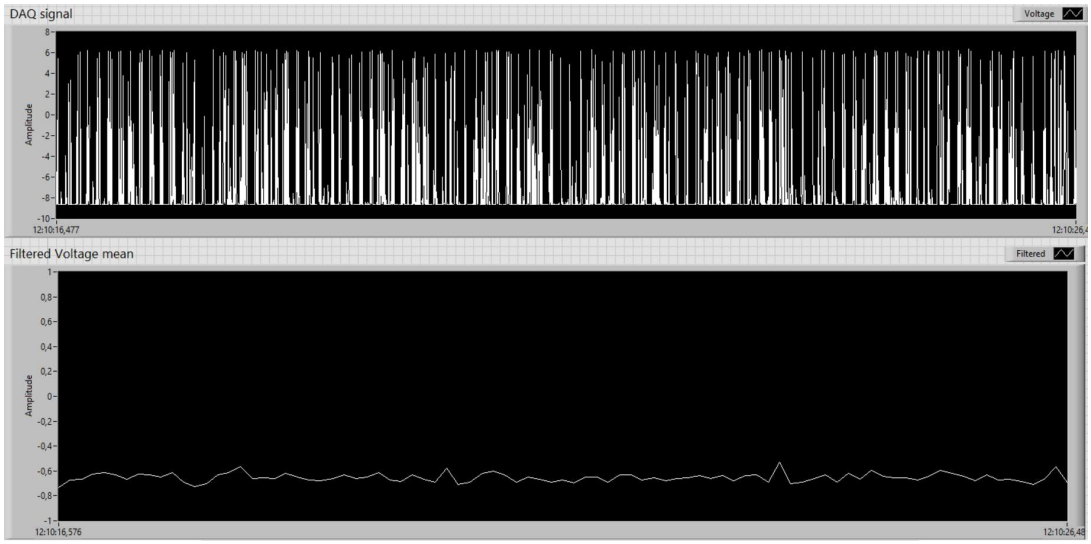

Figure 5.18: Display of the signal using an oscillatory frequency of 10 Hz

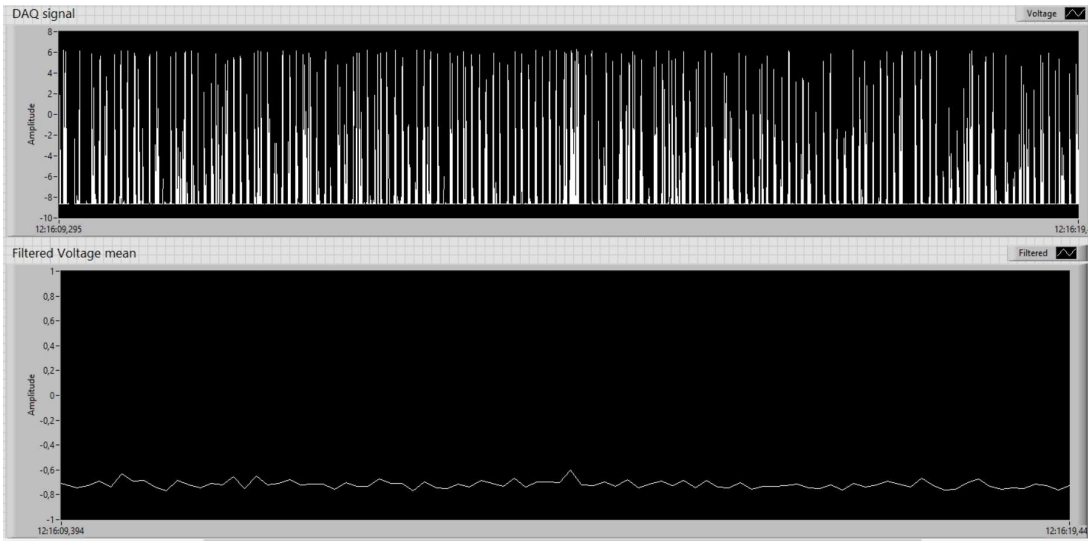

Figure 5.19: Display of the signal using an oscillatory frequency of 15 Hz

It can be clearly observed how the signal gradually loses its shape as the frequency of the oscillations is increased until reaching the maximum, where the signal gets almost flat. For this reason, it is necessary to take into account the sampling frequency of the processed signal (10 Hz) because according to the Nyquist theorem, for a proper reconstruction of the signal, the sampling frequency must be at least double the maximum frequency of the input signal.

6 Results

The results from the previous measurements are presented next in graph form in order to understand and analyse the behaviour of the capnometer under the different situations and obtain its characteristic calibration curve. Static characteristics of the signal are evaluated first from the static tests. Next, the results from the recorded signals with the device and with the reference capnometer are analysed and compared in order to establish some linear relation between the zero and $EtCO_2$ values read with the reference capnometer and the signal obtained from the designed device. Once the calibration is established, results from HFV tests are presented and analysed.

6.1 Analysis of zero input signal

The resulting graph of the zero input signal is presented in Figure 6.1 where it can be clearly observed how the signal is very close to be constant around -0,78 V.

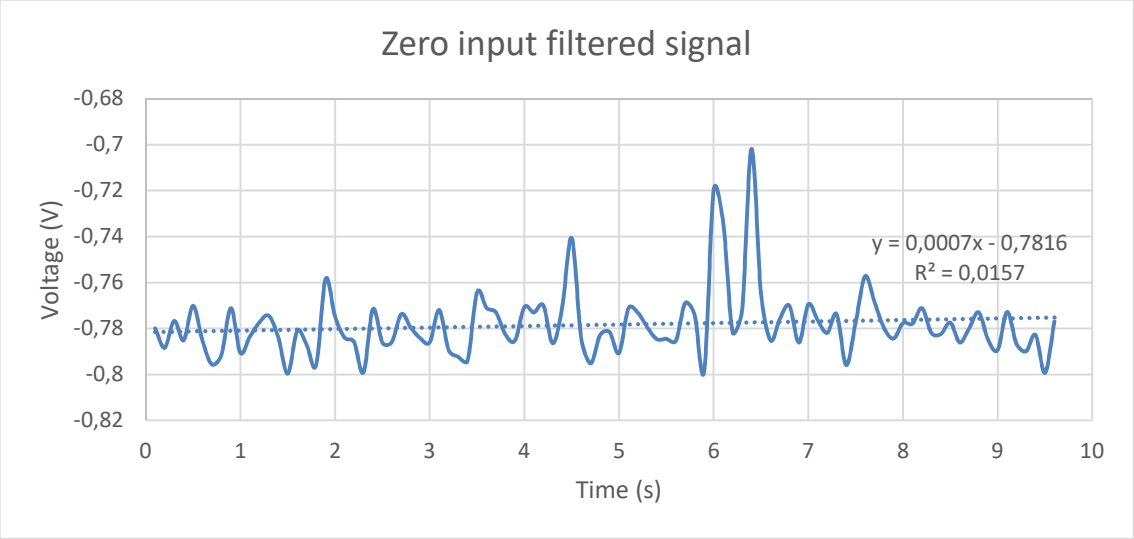

Figure 6.1: Zero input filtered signal graph (no airflow) graph with linear approximation equation and determination coefficient

The main values obtained from the previous graph are presented in Table 6.1

Table 6.1: Main voltage values obtained from the zero input signal

Maximum	- 0,701 V
Minimum	-0,799 V
Mean	-0,778 V
Standard Deviation	0,014 V
Quartile 1 25% of data is below this point	-0,785 V
Median 50% of data is below this point	-0,781 V
Quartile 3 75% of data is below this point	-0,772 V

Once the zero input signal is analysed and linearly averaged, the first relation between the voltage and the percentage of CO_2 can be established: an ambient CO_2 concentration of 0,03% (value confirmed by the reference capnometer) produced a voltage difference in the sensor of -0,778 ± 0,014 V.

6.2 Analysis of the step response signal

With the results of the next test, the step response of the system can be analysed as shown in Figure 6.2

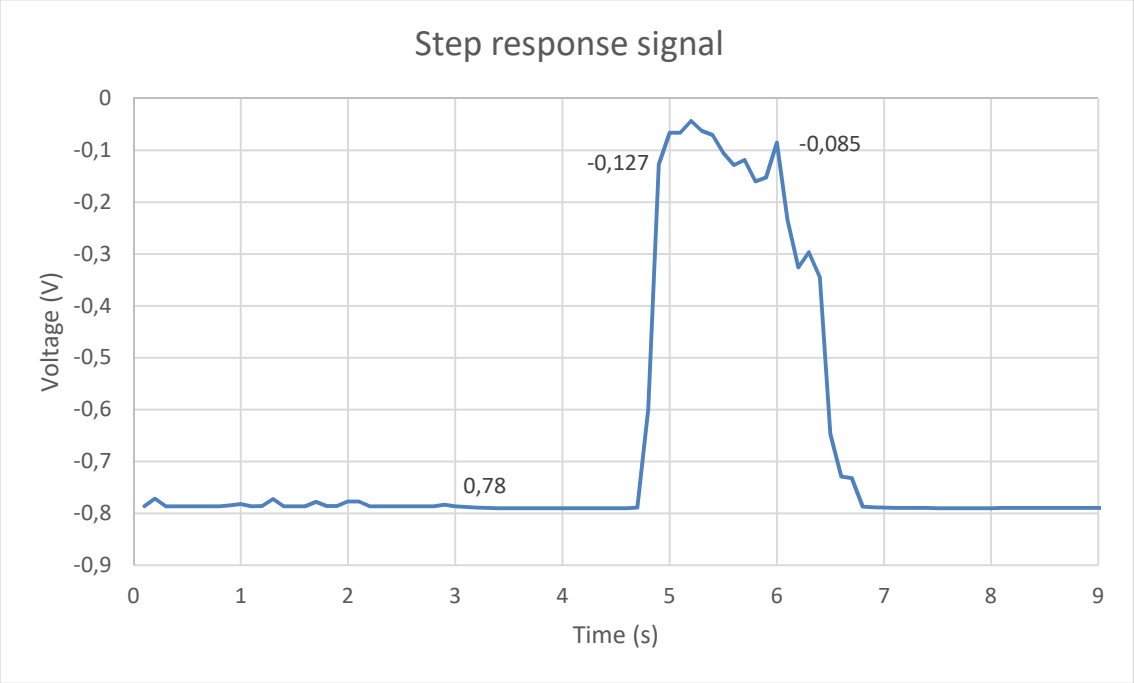

Figure 6.2: Step response signal graph (change from no airflow to CO_2 flow)

As expected, the more CO_2, the more absorption of IR, so less output voltage is produced by the detector. It is possible to verify that the zero input signal is established around -0,78 V and it goes up around -0,10 V when CO_2 is applied in a matter of ~ 0,20 s and producing a voltage difference of approximately 0,68 V. All these values are presented in table form in Table 6.2.

Table 6.2: Characteristics obtained from the step response signal

Response time of processed signal	~ 0,20 sec
Sampling frequency	10 Hz
Voltage difference produced (ΔV)	0,68 V
Voltage produced by baseline (no airflow)	-0,78 V
Voltage produced by CO_2 flow	- 0,10 V

6.3 Analysis of signals constant CO_2 and different flow rates

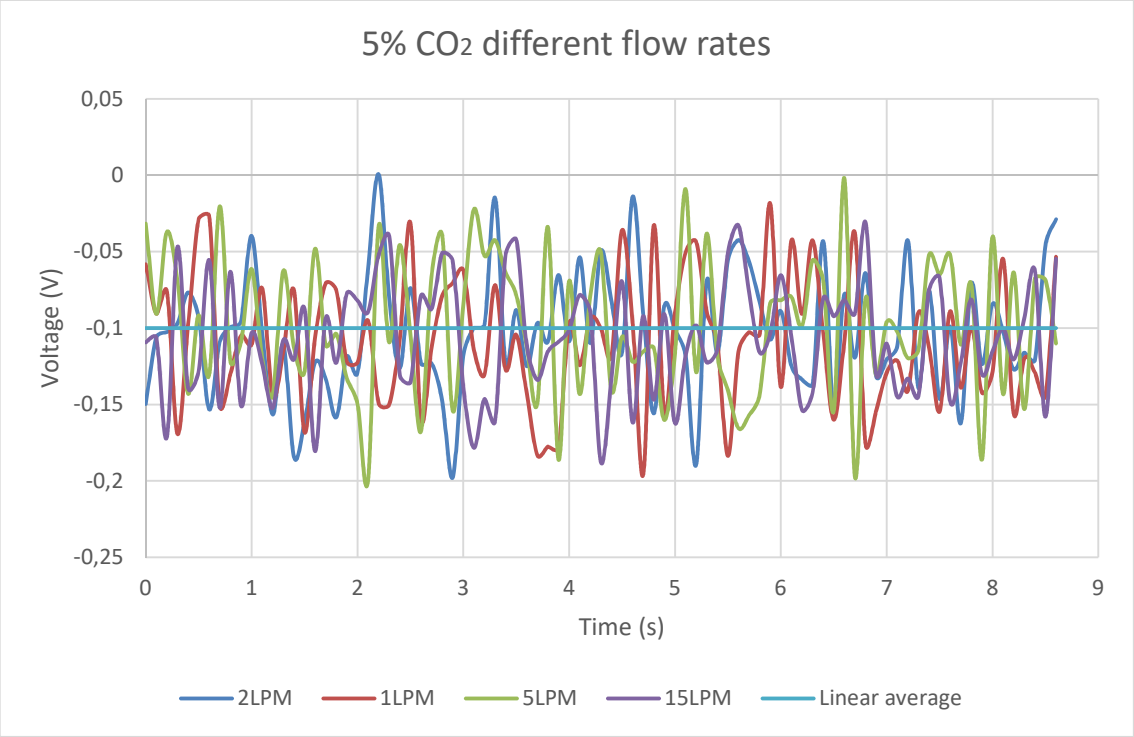

Figure 6.3: Overlapping of signals produced by constant 5% of CO_2 concentration using different flow rates (1, 2, 5 and 15 Lpm) with linear approximation

Table 6.3: Main values obtained from the 5% CO_2 input signal

Maximum	~ 0 V
Minimum	-0,224 V
Mean	-0,104 V
Standard Deviation	0,041 V
Quartile 1 25% of data is below this point	-0,125 V
Median 50% of data is below this point	-0,108 V
Quartile 3 75% of data is below this point	-0,078 V

It can be observed in Figure 6.3 that all the measurements performed using a constant concentration of 5% of CO_2 (measured with the reference capnometer) but different flow rates (1, 2, 5 and 15 litres per minute) gave very similar results. From these measurements, it is possible to observe the linear approximation of the signal which is constant around -0,10 V and with a ± 0,04 V of tolerance (from the standard deviation). After this experiment it is possible to verify that the flow rate is not affecting the output signal of the sensor, and it depends only on the concentration of CO_2 applied, which is a positive aspect of the device to note.

Once the static characteristics of the device with zero and constant CO_2 have being studied, it is possible to create a calibration curve that will correlate a voltage value with a specific CO_2 concentration. As mentioned in Chapter 2.1, the concentration of CO_2 in the exhaled air goes from ~ 3,8% to 5,0% (considered the maximum safe level concentration without health risks), any value over 5% would trigger the alarm of the CO_2 monitor. Thus, the range of CO_2 concentration to be read in capnography goes from 0 to 5% and this aspect must be considered in order to create an optimal calibration curve for this application.

6.4 Calibration curve

Combining the minimum and maximum CO_2 concentrations (read with the reference capnometer) with their respective voltages produced by the detector, it is possible to establish a linear relation between both as observed in Figure 6.4, where a CO_2 percentage of "x" will produce a voltage difference of "y" (V) according to the obtained equation (6). The red whiskers represent the tolerance region (± 0,04 V).

$$y = -0{,}1368x + 0{,}7841 \quad (6)$$

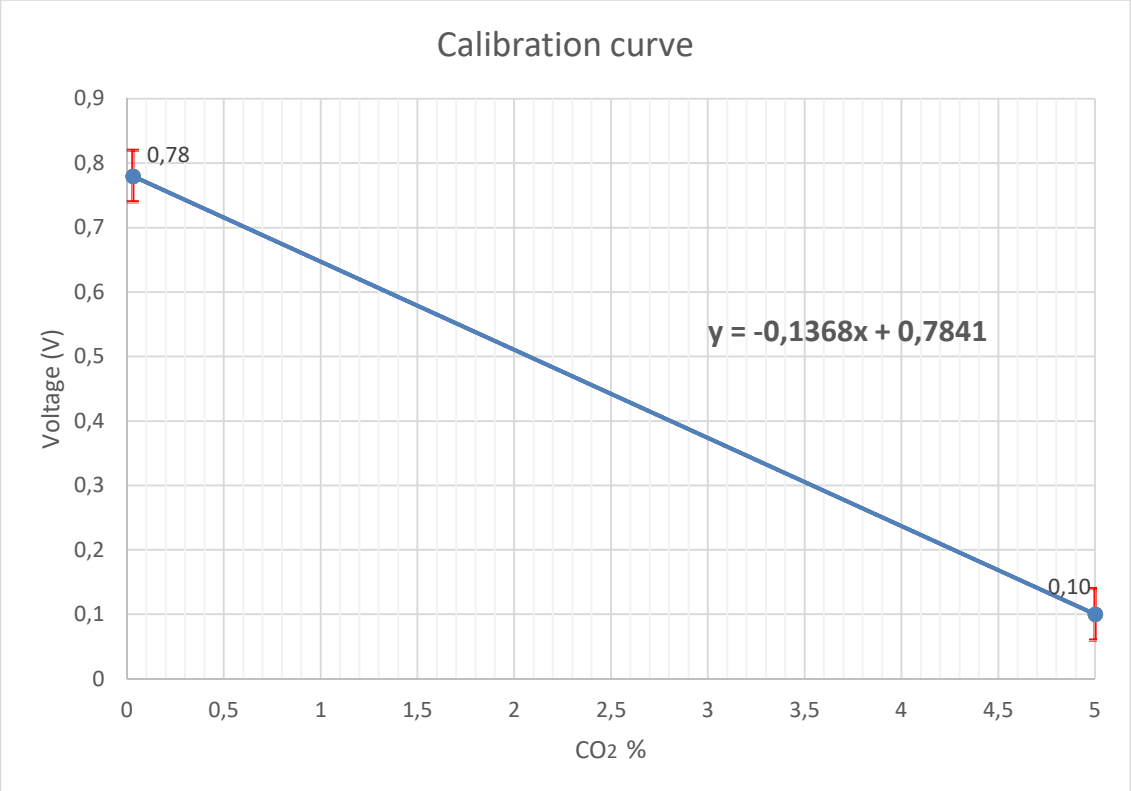

Figure 6.4: Linear calibration curve obtained from combination of the measurements

Table 6.4: Measured CO_2 and voltage obtained from reference and detector

CO_2 (%) from reference	Voltage (V) from detector
0,03 (min)	0,78
5 (max)	0,10

6.5 Analysis of normal breathing signal

In order to check the performance of the device and the accuracy of the obtained calibration curve for the designed capnometer, the same signal produced by normal breathing was recorded simultaneously together with the reference capnometer. The graph representing the signal displayed by the reference capnometer can be observed in Figure 6.5 and the one from the detector in Figure 6.6.

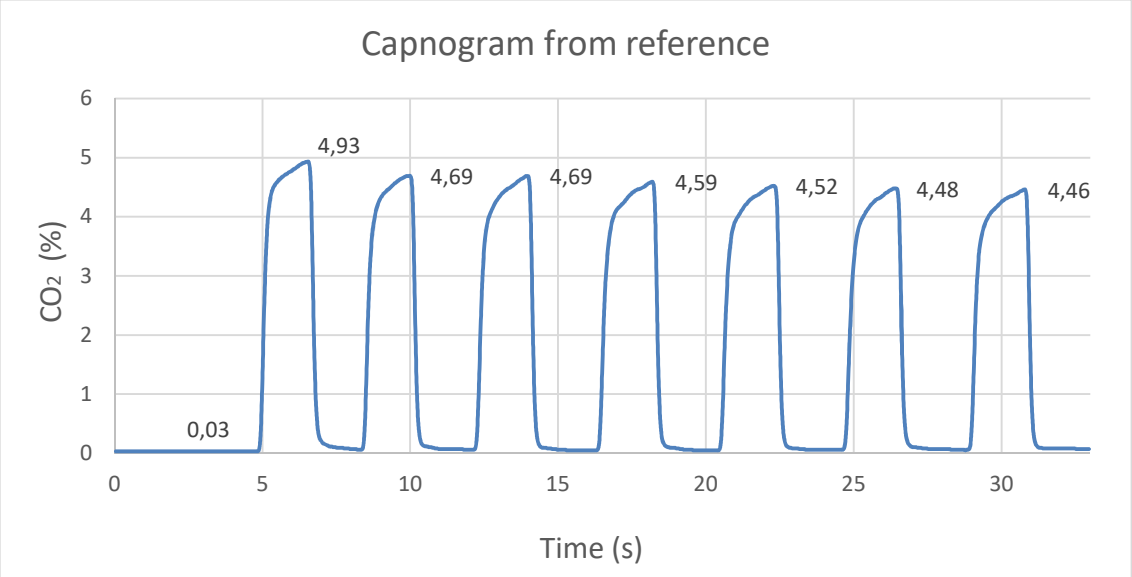

Figure 6.5: Capnogram recorded by reference capnometer with $EtCO_2$ values

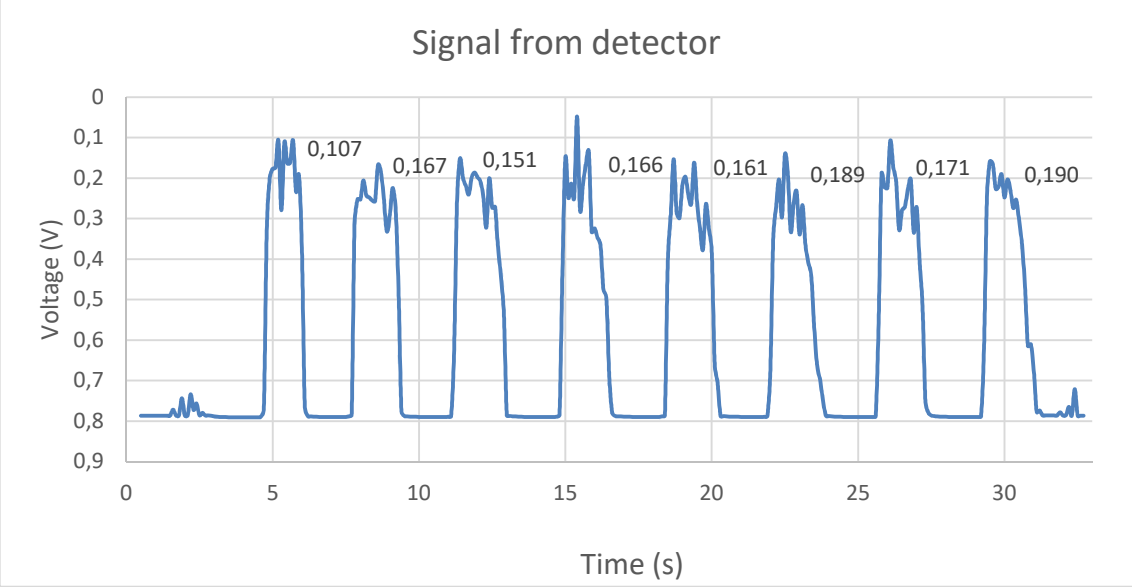

Figure 6.6: Signal produced by detector and voltage values corresponding to $EtCO_2$

Table 6.5: $EtCO_2$ from reference, measured voltage from detector and error

$EtCO_2$ (%)	**Voltage (V) measured from detector**	**Voltage (V) according to calibration curve**	**Error (ΔV)**
4,93	0,107	0,109	0,002
4,69	0,167	0,142	0,025
4,69	0,151	0,142	0,009
4,59	0,166	0,156	0,010
4,52	0,161	0,165	0,004
4,48	0,171	0,171	~ 0
4,46	0,190	0,173	0,017

The average error for the measurement of $EtCO_2$ values is approximately ± 0,001 V and the maximum was 0,01, which means that all the measured values are included in the region of tolerance of the calibration curve (± 0,04), confirming the high accuracy of the established linear relation between the carbon dioxide concentration and the produced voltage by the detector.

6.6 Analysis of HFV test

Last but not least, after the successful verification and calibration of the designed capnometer, it is possible to move on to the analysis of the results of the high frequency ventilator tests. The main goal of this tests was to verify if the device is able to follow accurately the CO_2 concentration signal when using frequencies associated with HFV.

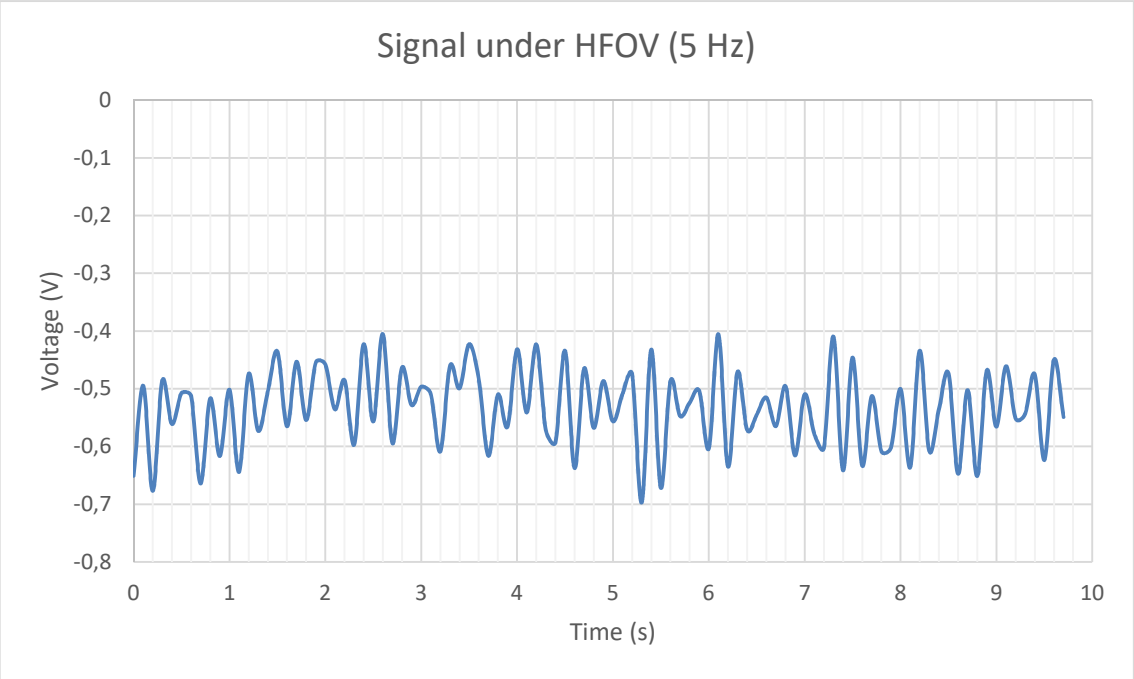

Figure 6.7: Signal obtained under HFOV, using an oscillatory frequency of 5Hz

In Figure 6.7, the resulting signal from the detector when applying 5 oscillations per second (5 Hz) can be clearly observed. It is also possible to verify that there are exactly 5 peaks in the signal for every second, confirming that the device is perfectly able to follow changes in the carbon dioxide concentration under this frequency. The chosen detector is able to produce signal with a sampling frequency of 50 Hz but the current implemented method to display the processed signal in the software uses a sampling frequency of 10 Hz. As mentioned in Chapter 5.3 and according to the Nyquist theorem, for a proper reconstruction of the signal, the sampling frequency must be at least double the maximum frequency of the input signal. Thus, theoretically, when using a sampling frequency of 10 Hz, the maximum frequency of the signal to be reconstructed should be 5 Hz or less. If this condition is not fulfilled, the aliasing effect will appear and the shape of the signal will be lost. Next, the rest of the signals with frequencies of 5.5, 6.0, 7.0, 10.0 and 15.0 Hz are presented from Figure 6.8 to Figure 6.12 respectively.

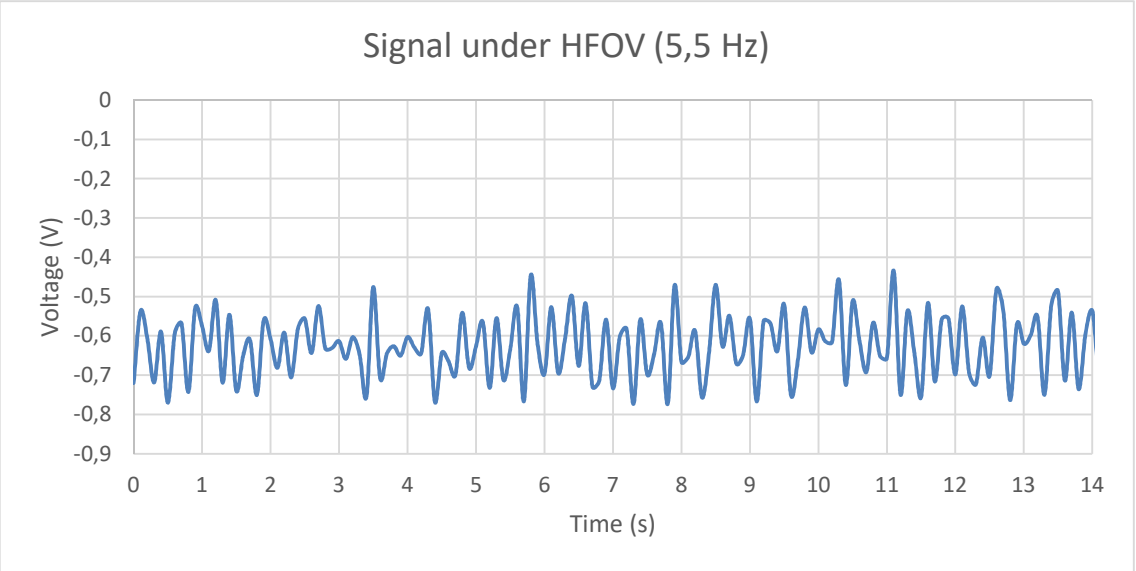

Figure 6.8: Signal obtained under HFOV, using an oscillatory frequency of 5,5 Hz

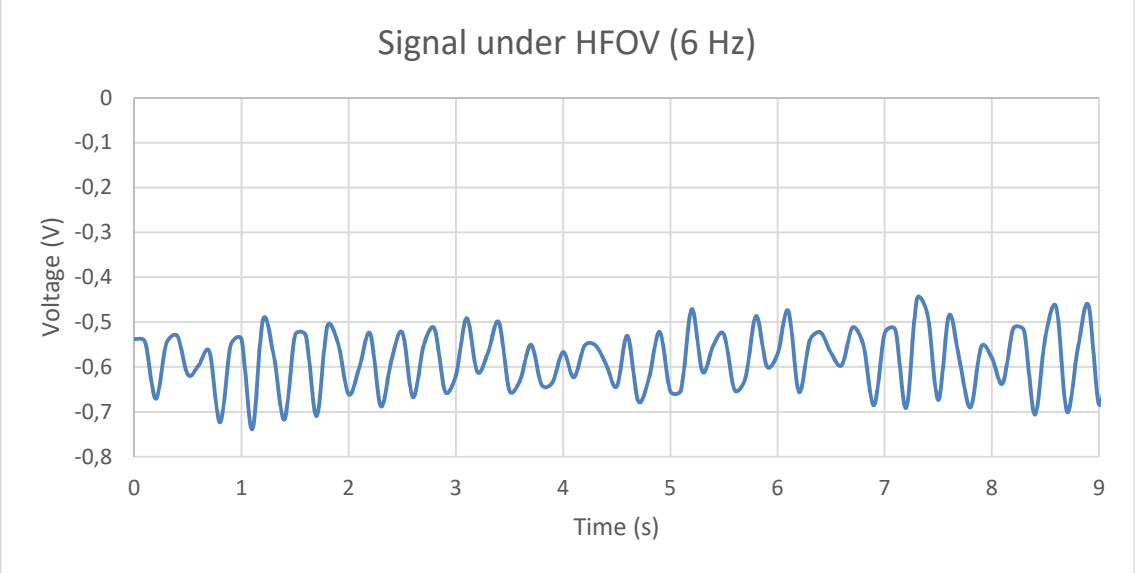

Figure 6.9: Signal obtained under HFOV, using an oscillatory frequency of 6 Hz

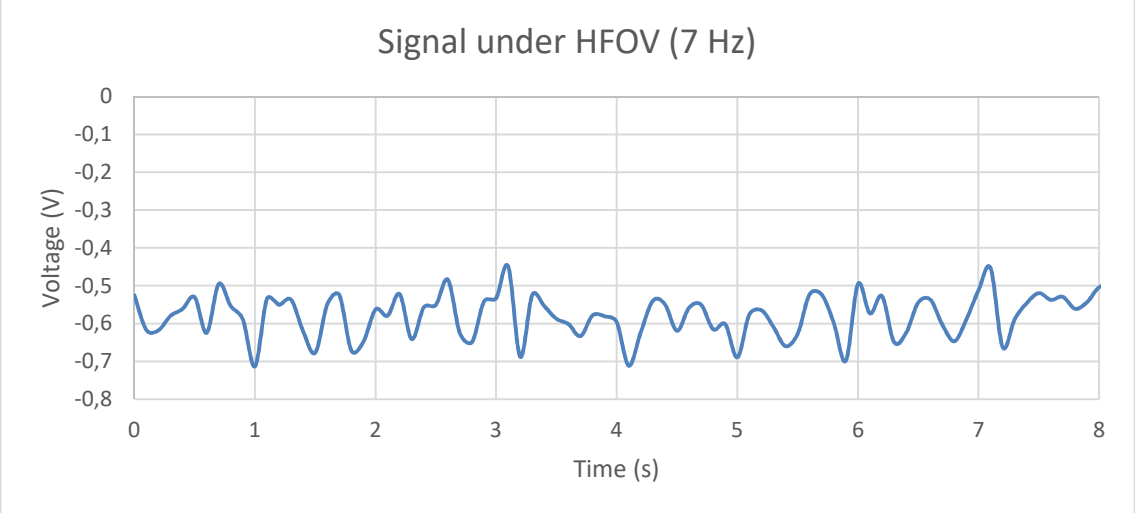

Figure 6.10: Signal obtained under HFOV, using an oscillatory frequency of 7 Hz

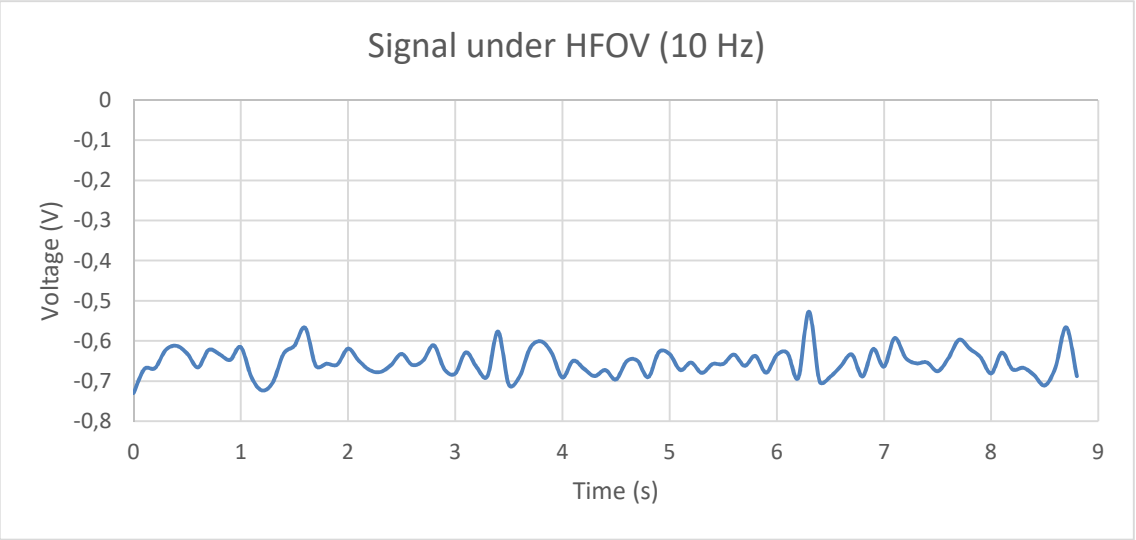

Figure 6.11: Signal obtained under HFOV, using an oscillatory frequency of 10 Hz

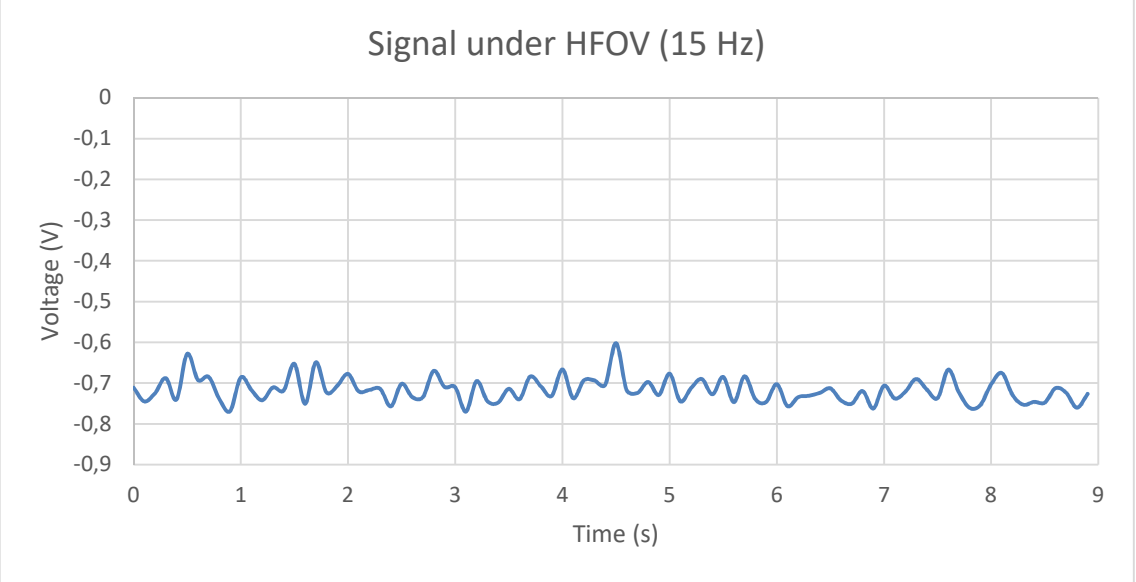

Figure 6.12: Signal obtained under HFOV, using an oscillatory frequency of 15Hz

As expected from the theoretical assumptions, the device is able to accurately process and display the oscillatory ventilator signal with frequencies up to 5 Hz. However, when further incrementing the frequency, it is possible to observe the existence of aliasing effect due to the mismatching of the number of peaks per second found in the signals and the set number of oscillations per second. It can be clearly observed how the signal loses its oscillatory shape and gets flat when incrementing the frequency over 5 Hz.

7 Discussion

During this chapter, main findings of this thesis are presented and analysed first according to the previously obtained results from the tests. Next, a comparison between the main characteristics of the designed device and one already commercialised (CAPNOSTAT 5) is presented.

The tests performed on the system allowed to identify its behaviour and main characteristics. The zero input test provided information about the static behaviour of the system under normal CO_2 level in the air, and the output voltage produced by the detector. The signal was stable, approximated as constant and linear around -0,78 V. Thus, first correlation between the CO_2 concentration and the output voltage produced was established. The step response test evaluated the time behaviour of the output when the percentage of CO_2 changed from 0 to 5 % in a very short time, where it was observed that the response time of the system is around 0,20 s producing a voltage difference of 0,68 V. The test with constant 5% of CO_2 and different flow rates allowed to verify that the flow rate does not influence on the output of the detector while the CO_2 concentration keeps constant, because the signals observed were almost identical, constant and linearized around -0,10 ± 0,04 V. The measured signals with known CO_2 concentration (from reference capnometer) used the maximum and minimum values that can be measured with capnography (from 0 to 5% CO_2) focusing on this specific range of detection for this specific application and optimizing the obtained calibration curve, were a percentage of CO_2 is correlated with the produced voltage.

The calibration curve was created simply by linear approximation ($y = -0,1368x + 0,7841$) and prove to be highly accurate when comparing the measured $EtCO_2$ values from reference capnometer and the ones obtained from the design, where the average error found was ± 0,001 V (or 0,1%) and the maximum error was ± 0,01 V (or 1%), being the region of tolerance of the calibration curve ± 0,04 V (or ± 4%), so every measured value was included in the tolerance region of the calibration curve.

During the implementation of the practical part of this project, there were some unexpected difficulties to achieve the successful functionality of the CO_2 detector. The first issue was to verify that the implemented circuit and each of its components were working adequately. Individual components of the circuit were checked and confirmed easily but once implemented together, the initial behaviour of the system was very unstable producing the output signal. This could be due to inadequate wire connexions, external interferences or inefficient setting of the circuit. However, to make the system more robust and stable, once the circuit was verified, it was mounted into a holder or plastic case.

Different methods were implemented in the software using LabVIEW to obtain the desired processed signal. The current implemented method uses simply a mean function generator (with a sampling frequency of 10 Hz) to process the raw signal, and it can clearly display the signal with changes in CO_2 concentration under normal breathing and conventional or even high frequency ventilation but it presents some limitations too.

The capnometer prove to be optimally usable in the neonatal breathing circuit under conventional and high frequency ventilation, being possible to increment the respiratory frequency until reaching 5 Hz. However, when using frequencies higher than 5 Hz, also associated to HFOV and HFJV, the output signal suffered from aliasing effect due to the inefficient sampling frequency of this implemented method for the processing of the signal. 10 samples per second (10 Hz) is not enough for respiratory rates higher than 300 bpm or 5 bps (5 Hz). With this assumption from the Nyquist sampling theorem (stated in previous chapters), it can be concluded that with the current implementation the device is able to accurately read up to 300 bpm, which is in the frequency range of HFOV and HFJV, thus, it could be used in this modes but not when the frequencies used are higher than 5 Hz. However, this limitation could be solved in further development by improving the current implemented method in the software or finding another one more optimal, that increases the sampling frequency of the processed signal at least in the order of 3 times (maximum respiratory frequency used in HFV is 15 Hz, and currently it uses a sampling frequency of 10 Hz so at least 30 Hz would be needed for optimal sampling).

Next, a comparison between the main characteristics of the design and a capnometer available in the market (CAPNOSTAT 5) is presented.

Comparison between commercialised and designed capnometer

The CAPNOSTAT 5 Sensor developed by Respironics (recognized as global leader in capnography) is the ideal capnography solution for patient monitoring. It provides technologically advanced measurement of $EtCO_2$, respiration rate, and a clear, accurate capnogram at all respiratory rates up to 150 breaths per minute. It is a flexible device as it can be used in either adults or neonates. It uses the same transducer type of the designed system (mainstream CO_2 sensor) and the same principle of operation (NDIR, single beam optics, dual wavelength, with no moving parts). Furthermore, it is compact and reliable. It is designed to be integrated into the patient monitoring system and it uses the very latest digital signal processor for reliable and flexible analogue-to-digital conversion. The main characteristic of the CAPNOSTAT 5 Sensor are presented and compared with the ones of the capnometer designed for this thesis in Table 7.1.

Table 7.1: Comparison of the main characteristics between the designed and commercialized capnometer CAPNOSTAT 5

Characteristic	**Capnostat 5** [52]	**Designed capnometer**
Operation mode	Integrated into monitor	Independent system
Transducer type	Mainstream CO_2 sensor	Mainstream CO_2 sensor
Principle of operation	NDIR, single beam, dual wavelength, no moving parts	NDIR, single beam, dual wavelength, no moving parts
CO_2 measurement range	0 to 19,7 %	0 to 5 %
Rise time	Less than 60 ms	0,20 s
CO_2 accuracy	±5 % of reading	±4 % of reading
Respiratory Rate range	0 to 150 bpm	0 to 300 bpm
Calibration	Not required	Preliminary calibrated Further calibration for clinical use
Voltage requirements	+5 V	+-10 V
Data output	Display takes 15 s CO_2 concentration, $EtCO_2$, Respiratory rate, capnography curve	Display in Real time Capnography curve CO_2 value by calibration curve

After the main characteristics of both capnometers have been compared, it is possible to highlight the advantages and disadvantages that they have over the other. While the CAPNOSTAT 5 has been designed to be integrated with most of the available monitors in the market (which is a great feature), the capnometer designed for this thesis works as independent system, so technically both can perform in clinical practice. However, the designed CO_2 sensor relies on some components that are external (not totally integrated into the capnometer case itself) for example the power source, the amplifier, the DAQ system, and the computer for the display of the results. For this reason, the CAPNOSTAT offers a better portability and it's more compact and stable device. Both use the same transistor type and operation principle (mainstream CO_2 sensor based on NDIR, with single beam, dual wavelength and no moving parts).

The strongest point of the designed capnometer over the CAPNOSTAT 5 is its ability to measure respiratory frequencies up to 300 breaths per minute, duplicating the maximum respiratory frequency that can be applied to the CAPNOSTAT 5. Preliminary calibration was done but ideally further calibration would be needed to be properly used in clinical practice, while CAPNOSTAT 5 does not need any additional calibration. Another advantage of the designed device is that the display of the current signal is in real time, it does not need any additional time to display the signal, while the CAPNOSTAT 5 takes up to 15 sec in displaying the results. Nevertheless, the final display and the results are much clear and reliable when using the CAPNOSTAT 5 and it present more different valuable information apart from the capnography curves, such as $EtCO_2$ values, and respiratory rate.

8 Conclusion

To conclude this thesis, after the complete evaluation of the results from the performed tests, it is possible to confirm that the designed prototype of the mainstream capnometer is able to perform accurate and real time measurements of CO_2 concentration changes in the neonatal breathing circuit during mechanical ventilation.

With the adequate selection of the components needed for the implementation of the system and subsequent verification, it was possible to integrate these components as a whole, open and independent functional system, permitting further development on it. The system performs continuous measurement of the CO_2 concentration changes, recording the data and transferring it to the computer for processing and final display of the signal.

The experiments performed for this thesis allowed the behaviour of the implemented capnometer to be analysed under different conditions and establish a linear relation specifically for the capnography reading range, where a specific percentage of CO_2 is related to the voltage difference that the detector will produce. The high accuracy of the linear approximation was proven by comparing measured and theoretical $EtCO_2$ values obtained from the calibration curve and from the reference capnometer. Moreover, the HFV tests allowed to verify the maximum frequency at which the device could be used, confirming its functionality under this mode.

From the comparison established between the designed and commercialised capnometer, it is possible to highlight the main advantages and disadvantages of the device´s features. In general it can be concluded that they have similar accuracy and performance but while CAPNOSTAT 5 displays more relevant data apart from the capnography curves, the designed capnometer is able to perform and display measurements much faster, at twice the maximum frequency used by CAPNOSTAT 5.

Currently, the maximum respiratory frequency that the device is able to read is 300 bpm or 5 Hz, therefore it can be used in conventional and HFV modes under this maximum frequency. Nevertheless, it could be increased even further in future development of the system. Moreover, the values presented in the graphs and displays are more or less informative and do not trace proper capnography curves with a value of useful information for the clinical practice, but they were suitable for the successful verification of the device´s functionality in conventional and high frequency ventilation modes. The whole work is analysed more from a design point of view and it would be appropriate to focus on the analysis of measured data and their specific use in clinical practice in further research.

References

[1] Ranney ML, Griffeth V, Jha AK. Critical Supply Shortages - *The Need for Ventilators and Personal Protective Equipment during the Covid-19 Pandemic.* N Engl J Med. 2020 Apr 30;382(18):e41. doi: 10.1056/NEJMp2006141. Epub 2020 Mar 25. PMID: 32212516.

[2] Haribhai S, Mahboobi SK. Ventilator Complications. [Updated 2021 Jan 29]. In: StatPearls [Internet]. Treasure Island (FL): StatPearls Publishing; 2021 Jan-. Available from: https://www.ncbi.nlm.nih.gov/books/NBK560535/

[3] Pandya NK, Sharma S. *Capnography And Pulse Oximetry.* [Updated 2020 Sep 5]. In: StatPearls [Internet]. Treasure Island (FL): StatPearls Publishing; 2021 Jan-. Available from: https://www.ncbi.nlm.nih.gov/books/NBK539754/

[4] SIOBAL, Mark S, 2016. Monitoring Exhaled Carbon Dioxide. *Respiratory Care* [online]. 1 October 2016. Vol. 61, no. 10, p. 1397 LP – 1416. DOI 10.4187/respcare.04919. Available from: http://rc.rcjournal.com/content/61/10/1397.abstract

[5] ROCHA, Gustavo, SOARES, Paulo, GONÇALVES, Américo, SILVA, Ana Isabel, ALMEIDA, Diana, FIGUEIREDO, Sara, PISSARRA, Susana, COSTA, Sandra, SOARES, Henrique, FLÔR-DE-LIMA, Filipa and GUIMARÃES, Hercília, 2018. Respiratory Care for the Ventilated Neonate. *Canadian Respiratory Journal*. 2018. Vol. 2018. DOI 10.1155/2018/7472964.

[6] HUTTMANN, Sophie E., WINDISCH, Wolfram and STORRE, Jan H., 2014. Techniques for the measurement and monitoring of carbon dioxide in the blood. *Annals of the American Thoracic Society*. 2014. Vol. 11, no. 4, p. 645–652. DOI 10.1513/AnnalsATS.201311-387FR.

[7] CUMMINS, Eoin P, STROWITZKI, Moritz J and TAYLOR, Cormac T, 2021. *Mechanisms and consequences of oxygen and carbon dioxide sensing in mammals*. 2021. P. 463–488. DOI 10.1152/physrev.00003.2019.

[8] Patel S, Miao JH, Yetiskul E, Anokhin A, Majmundar SH, 2021. *Physiology, Carbon Dioxide Retention*. 2021 Jan 4. In: StatPearls [Internet]. Treasure Island (FL): StatPearls Publishing; 2021 Jan–. PMID: 29494063.

[9] AMINIAHIDASHTI, Hamed, SHAFIEE, Sajad, ZAMANI KIASARI, Alieh and SAZGAR, Mohammad, 2018. Applications of End-Tidal Carbon Dioxide (ETCO2) Monitoring in Emergency Department; a Narrative Review. *Emergency (Tehran, Iran)* [online]. 2018. Vol. 6, no. 1, p. e5. DOI 10.22037/emergency.v6i1.19298. Available from:http://www.ncbi.nlm.nih.gov/pubmed/29503830%0Ahttp://www.pubmedcentral.nih.gov/articlerender.fcgi?artid=PMC5827051

[10] THEOPHANIDES, Theophile, 2012. Introduction to Infrared Spectroscopy. *Infrared Spectroscopy - Materials Science, Engineering and Technology*. 2012. No. May. DOI 10.5772/49106.

[11] YANG, Jiachen, CHEN, Bobo, BURK, Kyle, WANG, Haitao and ZHOU, Jianxiong, 2016. A mainstream monitoring system for respiratory CO2 concentration and gasflow. *Journal of Clinical Monitoring and Computing*. 2016. Vol. 30, no. 4, p. 467–473. DOI 10.1007/s10877-015-9739-y.

[12] ALI, Shahood and WALKER, Jason, 2014. Measurement of gas. *Anaesthesia and Intensive Care Medicine*

[13] HILLIER, S C and LERMAN, J, 1989. Mainstream Vs Sidestream Capnography in Anesthetized Infants and Children. *Anesthesiology*. 1989. Vol. 71, no. Supplement, p. A357. DOI 10.1097/00000542-198909001-00357.

[14] ELITE, Flotrak, 2012. Capnography Reference Handbook.

[15] HITRAN [online]. 2022. Available from: https://hitran.org/

[16] KUPNIK, Dejan and SKOK, Pavel, 2007. Capnometry in the prehospital setting: Are we using its potential? *Emergency Medicine Journal*. 2007. Vol. 24, no. 9, p. 614–617. DOI 10.1136/emj.2006.044081.

[17] RICHARDSON, Marina, MOULTON, Kristen, RABB, Danielle, KINDOPP, Shawn, PISHE, Tushar, YAN, Charles, AKPINAR, Ilke, TSOI, Bernice and CHUCK, Anderson, 2016. Capnography for Monitoring End-Tidal CO2 in Hospital and Pre-hospital Settings: A Health Technology Assessment. *Capnography for Monitoring End-Tidal CO2 in Hospital and Pre-hospital Settings: A Health Technology Assessment* [online]. 2016. No. March. Available from: http://www.ncbi.nlm.nih.gov/pubmed/27227208

[18] LOPEZ, Emmanuel, GRABAR, Sophie, BARBIER, Alexandre, KRAUSS, Baruch, JARREAU, Pierre Henri and MORIETTE, Guy, 2009. Detection of carbon dioxide thresholds using low-flow sidestream capnography in ventilated preterm infants. *Intensive Care Medicine*. 2009. Vol. 35, no. 11, p. 1942–1949. DOI 10.1007/s00134-009-1647-5.

[19] WALSH, Brian K., CROTWELL, David N. and RESTREPO, Ruben D., 2011. Capnography/Capnometry during mechanical ventilation: 2011. *Respiratory Care*. 2011. Vol. 56, no. 4, p. 503–509. DOI 10.4187/respcare.01175.

[20] LIN, Hsin Ju, HUANG, Ching Tzu, HSIAO, Hsiu Feng, CHIANG, Ming Chou and JENG, Mei Jy, 2017. End-tidal carbon dioxide measurement in preterm infants with low birth weight. *PLoS ONE*. 2017. Vol. 12, no. 10, p. 1–10. DOI 10.1371/journal.pone.0186408.

[21] MARSHALL, Melissa, 2004. Capnography in dogs. *Compendium on Continuing Education for the Practicing Veterinarian*. 2004. Vol. 26, no. 10, p. 761

[22] JAFFE, Michael B, 1970. Mainstream or Sidestream Capnography?1970. P.1–14.

[23] HERRY, C L, TOWNSEND, D, GREEN, G C, BRAVI, A and SEELY, A J E, 2014. Segmentation and classification of capnograms : application in respiratory variability analysis.

[24] HERRY, C L, TOWNSEND, D, GREEN, G C, BRAVI, A and SEELY, A J E. *Segmentation and classification of capnograms : application in respiratory variability analysis.*

[25] DONOSO, Alejandro, ARRIAGADA, Daniela, CONTRERAS, Dina, ULLOA, Daniela and NEUMANN, Megan, 2017. Respiratory monitoring of pediatric patients in the Intensive Care Unit Intensive Care Unit [online]. 2017. No. October. DOI 10.1016/j.bmhime.2017.09.001. Available from: http://dx.doi.org/10.1016/j.bmhime.2017.09.001

[26] BHAVANI-SHANKAR, K and FFARCS, H Moseley, 1992. Review Article Capnometry and anaesthesia.

[27] GENDERINGEN H R, Gravenstein N, van der Aa J J & Gravenstein J S 1987 Computer-assisted capnogram analysis J Clin Monit 3(3), 194–200.

[28] COLBY, Christopher E. and HARRIS, Malinda N., 2017. Intraoperative Management of the Neonate. *Assisted Ventilation of the Neonate: An Evidence-Based Approach to Newborn Respiratory Care: Sixth Edition*. 2017. P. 407-415.e2. DOI 10.1016/B978-0-323-39006-4.00037-5.

[29] MEDTRONIC. [online]. 2022. Adapted from: https://www.medtronic.com/us-en/index.html

[30] FACKLER, James and MONITTO, Constance L, 2016. Pediatric Patients Treated With Patient-Controlled Analgesia. . 2016. Vol. 25, no. 10, p. 1054–1059. DOI 10.1111/pan.12702.Long-term.

[31] MUÑOZ JI. Conceptos de ventilación mecánica [Definitions in mechanical ventilation]. An Pediatr (Barc). 2003 Jul;59(1):60-6. Spanish. doi: 10.1016/s1695-4033(03)78150-8. PMID: 13678060.

[32] AK AK, Anjum F. Ventilator-Induced Lung Injury (VILI) [Updated 2021 Dec 15]. In: StatPearls [Internet]. Treasure Island (FL): StatPearls Publishing; 2022 Jan-. Available from: https://www.ncbi.nlm.nih.gov/books/NBK563244/

[33] GRIFFITHS, Mark J.D., MCAULEY, Danny Francis, PERKINS, Gavin D., BARRETT, Nicholas, BLACKWOOD, Bronagh, BOYLE, Andrew, CHEE, Nigel, CONNOLLY, Bronwen, DARK, Paul, FINNEY, Simon, SALAM, Aemun, SILVERSIDES, Jonathan, TARMEY, Nick, WISE, Matt P. and BAUDOUIN, Simon V., 2019. Guidelines on the management of acute respiratory distress syndrome. *BMJ Open Respiratory Research*. 2019. Vol. 6, no. 1. DOI 10.1136/bmjresp-2019-000420.

[34] ACKERMANN, Benjamin W., KLOTZ, Daniel, HENTSCHEL, Roland, THOME, Ulrich H. and VAN KAAM, Anton H., 2022. High-frequency ventilation in preterm infants and neonates. *Pediatric Research*. 2022. No. January. DOI 10.1038/s41390-021-01639-8.

[35] Mutz N, Baum M, Benzer H, Putz G. *Clinical experience with several types of high frequency ventilation*. Acta Anaesthesiol Scand Suppl. 1989;90:140-4. doi: 10.1111/j.1399-6576.1989.tb03020.x. PMID: 2648733.

[36] Murthy PR, AK AK. *High Frequency Ventilation.* [Updated 2021 Jul 30]. In: StatPearls [Internet]. Treasure Island (FL): StatPearls Publishing; 2022 Jan-. Available from: https://www.ncbi.nlm.nih.gov/books/NBK563151/

[37] MIRELES-CABODEVILA, Eduardo, DIAZ-GUZMAN, Enrique, HERESI, Gustavo A. and CHATBURN, Robert L., 2009. Alternative modes of mechanical ventilation: A review for the hospitalist. *Cleveland Clinic Journal of Medicine*. 2009. Vol. 76, no. 7, p. 417–430. DOI 10.3949/ccjm.76a.08043.

[38] MEYERS, Morgan, RODRIGUES, Nathan and ARI, Arzu, 2019. High-frequency oscillatory ventilation: A narrative review. 2019.]

[39] VAN HEERDE, Marc, ROUBIK, Karel, KOPELENT, Vitek, PLÖTZ, Frans B. and MARKHORST, Dick G., 2006. Unloading work of breathing during high-frequency oscillatory ventilation: A bench study. Critical Care. 2006. Vol. 10, no. 4. DOI 10.1186/cc4968.

[40] MILLER, Andrew G, BARTLE, Renee M and REHDER, Kyle J, 2021. High-Frequency Jet Ventilation in Neonatal and Pediatric Subjects: A Narrative Review. *Respiratory Care* [online]. 1 May 2021. Vol. 66, no. 5, p. 845 LP – 856. DOI 10.4187/respcare.08691. Available from: http://rc.rcjournal.com/content/66/5/845.abstract

[41] CARPI, Mário Ferreira, 2017. High-frequency jet ventilation in preterm infants: Is there still room for it? *Respiratory Care*. 2017. Vol. 62, no. 7, p. 997–998. DOI 10.4187/respcare.05647.

[42] KEMH, Nicu, PCH, Nicu and WA, Nets, [no date]. Ventilation : High Frequency Jet Ventilation (HFJV) Child Safe Organisation Statement of Commitment. No. Cv.

[43] BUNNELL, J Bert and SC, D. High-Frequency Jet Ventilation of Infants and Children.]

[44] BOROS, et al. *Comparison of high-frequency oscillatory ventilation and high-frequency jet ventilation in cats with normal lungs*. Pediatr Pulmonol. 1989;7(1):35-41. doi: 10.1002/ppul.1950070109. PMID: 2771469.

[45] Di Cicco et al. 2021. Structural and functional development in airways throughout childhood: Children are not small adults. *Pediatric Pulmonology*. Vol. 56, no. 1, p. 240–251. DOI 10.1002/ppul.25169.

[46] ALEX YARTSEV. *Neonatal respiratory physiology | Deranged Physiology*. June, 2015]

[47] HODGKINSON, Jane, SMITH, Richard, HO, Wah On, SAFFELL, John R. and TATAM, Ralph P., 2013. *Non-dispersive infra-red (NDIR) measurement of carbon dioxide at 4.2 μm in a compact and optically efficient sensor*. Sensors and Actuators, B: Chemical. 2013. Vol. 186, no. September, p. 580–588. DOI 10.1016/j.snb.2013.06.006.

[48] HAMAMATSU P13243-043MF, 2022. [online]. Available from: https://www.hamamatsu.com/eu/en/product/optical-sensors/infrared-detector/inassb-photovoltaic-detector/P13243-043MF.html

[49] HAMAMATSU P13243-039MF, 2022. [online]. Available from: https://www.hamamatsu.com/eu/en/product/type/P13243-039MF/index.html

[50] HAMAMATSU T11722-01, 2022. [online]. Available from: https://www.hamamatsu.com/eu/en/product/type/T11722-01/index.html

[51] DAQ SYSTEM, 2022. [online]. Available from: https://es.wikipedia.org/wiki/Adquisición_de_datos

[52] RESPIRONICS, 2007. Capnostat 5 Mainstream Co 2 Sensor. Philips [online]. 2007. P. 2–3. Available from: http://www.oem.respironics.com/Downloads/01-1742-4101194-Capnostat.pdf

Appendix

List of Figures

List of Tables

List of files included in online submission

Excel files

Calibration curve

Constant CO_2 and different flow rates

Capnogram signal recorded by detector

Capnogram recorded by reference capnometer

Detector zero input signal

Detector step response

Detector signals under HFV

LabVIEW Instrument file

Capnometer signal display